# $\Psi_k$ Newsletter

## AB INITIO (FROM ELECTRONIC STRUCTURE) CALCULATION OF COMPLEX PROCESSES IN MATERIALS

Number 96 December 2009


Editor: Z (Dzidka) Szotek
E-mail: psik-coord@dl.ac.uk

Sponsored by: UK's CCP9 and Psi-k

# Contents


**1 Editorial** **4**

**2 General News** **5**

2.1 $\Psi_k$ Conference 2010 . . . . . 5

**3 Psi-k Activities** **7**

3.1 Reports on the Workshops supported by Psi-k . . . . . 7

3.1.1 Report on International Workshop "Quantum Monte Carlo in the Apuan Alps V" . . . . . 7

3.1.2 Report on International Summer School "Quantum Monte Carlo and the CASINO program IV" . . . . . 12

3.1.3 Report on the $14^{th}$ ETSF Workshop on Electronic Excitations: Ab-initio tools for the characterization of nanostructures . . . . . 15

3.1.4 Report on Workshop Computer Simulation of Oxides: Dopants, Defects and Surfaces . . . . . 23

3.1.5 Report on the CECAM workshop"Which electronic structure method for the study of defects?" . . . . . 32

**4 General Workshop/Conference Announcements** **37**

4.1 International Workshop on Quantum Monte Carlo in the Apuan Alps VI . . . . . 37

4.2 Summer School on Quantum Monte Carlo and the CASINO program V . . . . . 38

**5 Abstracts** **40**

**6 Presenting Other Initiatives** **48**

6.1 First Official Release of the Exciting Code . . . . . 48

**7 SCIENTIFIC HIGHLIGHT OF THE MONTH: "Electrical Polarization and Orbital Magnetization: The Modern Theories"** **49**

**1 Introduction** **50**

**2 Macroscopics** **51**

2.1 Fundamentals . . . . . 51

2.2 Finite samples and shape issues . . . . . 52

**3 Microscopics** **55**

**4 DFT, pseudopotentials, and more** **56**

**5 Linear response** **57**

5.1 Linear-response tensors . . . . . 58

5.2 Electrical case: pyroelectricity, piezoelectricity, and IR charges . . . . . 59

5.3 A closer look at IR charges (Born effective charge tensors) . . . . . 59

5.4 Magnetic case: NMR shielding tensor . . . . . 60

**6 Modern theory of polarization** **61**

6.1 Single **k**-point formula for supercell calculations . . . . . 62

6.2 Many **k**-point formula for crystalline calculations . . . . . 63

6.3 King-Smith & Vanderbilt formula . . . . . 65

6.4 The polarization "quantum" . . . . . 65

6.5 Wannier functions . . . . . 66

**7 Geometrical issues** **67**

7.1 Chern invariants and topological insulators . . . . . 67

7.2 Berry curvature and the anomalous Hall effect . . . . . 69

**8 Modern theory of magnetization** **70**

8.1 Normal insulators . . . . . 70

8.2 Single **k**-point formula for supercell calculations . . . . . 71

8.3 Chern insulators and metals . . . . . 73

8.4 Finite-temperature formula . . . . . 74

8.5 Transport . . . . . 75

8.6 Dichroic $f$-sum rule . . . . . 75

**9 Conclusions** **76**

**10 Acknowledgments** **77**

# 1 Editorial

This last newsletter of 2009 is started with the updated information on the forthcoming Psi-k Conference in 2010. This is followed by a number of workshop reports, workshop/school announcements, and abstracts of newly submitted or recently published papers. After the abstracts, in the section "Presenting Other Initiatives" we have a short information on the first official release of the Exciting Code.

A very impressive scientific highlight of this newsletter is by Raffaele Resta (Trieste) on "Electrical Polarization and Orbital Magnetization: The Modern Theories".

For further details please check the table of content of this newsletter.

The *Uniform Resource Locator* (URL) for the Psi-k webpage is:

**http://www.psi-k.org.uk/**

**Please submit all material for the next newsletters to the email address below**

psik-coord@dl.ac.uk.

Since it is the last newsletter of this calendar year, we would like to wish all our readers

**Merry Christmas and a very Happy New Year!**


Dzidka Szotek, Martin Lüders and Walter Temmerman
e-mail: psik-coord@dl.ac.uk

# 2 General News

## 2.1 $\Psi_k$ Conference 2010

**Henry Ford Building, Berlin, Germany**

**September 12 - 16, 2010**

Conference Web Page:
`http://www.fhi-berlin.mpg.de/th/Meetings/psik_2010/`

Conference Chair: Matthias Scheffler
Co-Chair: Hardy Gross
Honorary Chair: Volker Heine

Program Committee
Matthias Scheffler - Chair (Berlin, Germany)
Peter Dederichs - Vice-Chair (Jlich, Germany)
Walter Temmerman - Vice-Chair (Daresbury, United Kingdom)

This is just to update you on the forthcoming Psi-k2010 Conference which will take place next year in Berlin. Like the three previous Psi-k conferences (1996, 2000, 2005), the forthcoming conference will cover theoretical and computational research on electronic structure and properties of matter, ranging from novel basic concepts and methods to applications for condensed matter and real functional materials to systems of biological interest. All the up to date information on the Psi-k2010 conference can be found on the official conference web page given above.

Most importantly, the five plenary talks of the conference will be given by

Stefano Baroni (Trieste)
Gerbrand Ceder (Boston)
Jens Norskov (Lyngby)
Mark Ratner (Evanston)
David Vanderbilt (Piscataway).

The conference will be run in four parallel sessions, with 21 symposia and about 110 invited speakers. Among the speakers there are such well known names as Marvin Cohen (Berkeley), John Perdew (Tulane), Michele Parrinello (Manno), Warren Pickett (Davis), Gustavo Scuseria (Houston), David Singh (Oak Ridge), Jose Soler (Madrid), Alex Zunger (Golden), and many others, as given at the above conference web page.

The themes of the symposia are:

Climbing Jacob's Ladder: from Local Functionals to Wavefunction based Methods
Electronic Excitations
Strong Correlation from First Principles
Recent Developments in Dynamical Mean-Field Theory
Quantum Monte Carlo
Superconductivity
Linear-Scaling and Large-Scale DFT
First-Principles based Multi-Scale Modeling
Multiferroics and Oxides
Magnetism and Spintronics
Crystalline, Amorphous, and Glassy Alloys
Earth and Planetary Materials and Matter at Extreme Conditions
Solid-Solid and Solid-Liquid Interfaces
Solar Energy Conversion and Harvesting
Organic Electronics
Nanoscale Structures and Phenomena
Surface Science, Catalysis and Energy Conversion
Ab Initio Modeling of Biological Systems
Transport
Quantum Dynamics
Exploiting Advanced Computing Architectures
Vibrational Coupling

The important dates are:

* Registration and abstract submission open: Dec 1, 2009
* Abstract submission deadline: May 1, 2010
* Deadline for support applications: May 1, 2010
* Early registration deadline: June 1, 2010

For further details please check the conference web page.

# 3 Psi-k Activities

## "Towards Atomistic Materials Design"

### 3.1 Reports on the Workshops supported by Psi-k

#### 3.1.1 Report on International Workshop "Quantum Monte Carlo in the Apuan Alps V"

Saturday 25th July - Saturday 1st August 2009
The Apuan Alps Centre for Physics @ TTI, Vallico Sotto, Tuscany
`www.vallico.net/tti/tti.html`

Sponsors: Psi-k, CCP9
Organizer: Mike Towler
Conference web page: `www.vallico.net/tti/qmcitaa_09/conference.html`

The fifth Cambridge international workshop devoted to the Quantum Monte Carlo (QMC) method took place in late July 2009. The event was organized and run by Mike Towler of Cambridge University, and was held in the pleasant setting of his 15th century monastery in the beautiful mountain village of Vallico Sotto in Tuscany. Workshops at this venue are generally intended to gather together limited numbers of expert physicists to discuss subjects of topical interest where there is an ongoing requirement for new insights. This workshop - like the previous four - appeared to be succeed very well in its stated purpose, and all participants enjoyed a varied programme of interesting lectures and discussions.

The quantum Monte Carlo method is an important and complementary alternative to density functional theory when performing computational electronic structure calculations in which high accuracy is required. The method has many attractive features for probing the electronic structure of real atoms, molecules and solids. In particular, it is a genuine many-body theory with a natural and explicit description of electron correlation which gives consistent, highly-accurate results while at the same time exhibiting favourable (cubic or better) scaling of computational cost with system size. It is the *only* known highly-accurate method which remains tractable for systems with more than a few tens of electrons; indeed, solid-state applications of more than 2000 electrons were reported during the workshop.

Here is a (by no means exhaustive) list of interesting themes presented and discussed at this year's event:

- Insights into QMC and other numerical simulations from trajectory-based interpretations of quantum mechanics (specifically, de Broglie-Bohm pilot-wave theory)

- Various new forms of many-particle wave function, including a new completely general form of Jastrow correlation factor which allows the inclusion of arbitrary higher-order terms.
- QMC calculation of weak interactions.
- The exploitation of new petascale parallel hardware to do quantum Monte Carlo calculations.
- Forces and the optimization of geometries in QMC.
- A completely new algorithm for doing QMC in a 'Slater determinant space'.
- A very wide-range of applications of QMC to atoms, molecules, surfaces, solids and various model systems.

As is usual with events at this venue, formal lectures were restricted to the mornings, and participants were encouraged to spend the remainder of each day thinking about and discussing the topics at hand. For those so inclined, a wide variety of activities were organized for each afternoon, often involving mountain walks and cave exploration.

## Programme

```
Sunday 26th July
----------------
8.30am  : Mike Towler (5 minutes)
        - "Welcome to Tuscany"
8.35am  : Mike Towler (50 minutes)
        - "Pilot waves, Feynman path integrals, and quantum Monte Carlo"
9.30am  : Dario Alfe (50 minutes)
        - "Water graphene binding energy curve from diffusion Monte Carlo"
10.30am : Pablo Lopez Rios (50 minutes)
        - "The Jastrow factor"
11:30am : Richard Needs (50 minutes)
        - "Applications of ab initio random structure searching"

Monday 27th July
----------------
8.30am  : Michele Casula (50 minutes)
        - "Hexatic and mesoscopic phases in the 2D quantum Coulomb system"
9.30am : Ken Esler (50 minutes)
        - "Recent developments in QMC for periodic systems"
10:30am : Alston Misquitta (50 minutes)
        - "The dispersion energy: an introduction and some surprises"
11.30 am: Martin Krupicka (25 minutes)
```

- "Comparison of QMC and ab initio methods for eight constitutional
  isomers of C4H6"

Tuesday 28th July
---
8.30am : Lucas Wagner (50 minutes)
- "Using QMC to optimize geometries"
9.30am : Matthew Foulkes (50 minutes)
- "Point defects and diffusion in alumina"
10.30am : Roberto Dovesi (50 minutes)
- "State of the art in the ab initio treatment of crystalline solids
  with a local basis set. The case of the CRYSTAL code, and its CRYSCOR son"
11.30am : Mariapia Marchi (25 minutes)
- "Resonating Valence Bond wave function with molecular orbitals:
  application to diatomic molecules"

Wednesday 29th July
---
8.30am : Shiwei Zhang (50 minutes)
- "Is the homogeneous electron gas homogeneous?"
9.30am : Neil Drummond (50 minutes)
- "Quasiparticle effective mass of the 2D homogeneous electron gas"
10.30am : Ching-Ming Wei (50 minutes)
- "QMC studies of (i) transition metal clusters, and (ii) surface adsorption".
11.30am : Robert Lee (25 minutes)
- "QMC and the 1d electron liquid"

Thursday 30th July
---
8.30am : Michel Caffarel (50 minutes)
- "A new type of trial wave function for electronic structure
  calculations with QMC"
9.30am : Norbert Nemec (50 minutes)
- "Diffusion Monte Carlo: exponentially inefficient for large systems"
10.30am : George Booth (50 minutes)
- "Quantum Monte Carlo in a discrete space"
11.30am : Martin Korth (50 minutes)
- "'Mindless' QMC benchmarking"

Fri 31st July
---
8.30am : John Trail (50 minutes)

```
        - "Optimum and efficient sampling for variational quantum Monte Carlo"
9.30am : Ryo Maezono (25 minutes)
        - "DMC study of an atom immersed in a jellium sphere"

10am : Andrew Morris (50 minutes)
        - "BEC-BCS crossover in ultracold atomic gasses within Quantum Monte Carlo"
11am :  Priyanka Seth (25 minutes)
        - "QMC studies of the first row atoms"
11.30am : Gareth Griffiths (25 minutes)
        - "Post-cotunnite phase of TeO2 from random structure searching"

Poster presentation
-------------------
Raffaella Dimichelis
"Ab initio quantum mechanical simulation of systems with helical symmetry:
  carbon and chrysotile nanotubes"
```

All presentations should be downloadable from the conference web site.

## List of participants

There were 28 scientific participants in the meeting from 7 countries, accompanied by 12 family members. Their names and affiliations were as follows:

Dario Alfè (UCL, London, U.K.)
George Booth (Cambridge University, U.K.)
Michel Caffarel (Université Pierre et Marie Curie, Paris, France)
Michele Casula (Ecole Polytechnique, Paris, France)
Raffaella Demichelis (University of Torino, Italy)
Roberto Dovesi (University of Torino, Italy)
Neil Drummond (Cambridge University, U.K.)
Ken Esler (University of Illinois, U.S.A.)
Matthew Foulkes (Imperial College, London, U.K.)
Gareth Griffiths (Cambridge University, U.K.)
Bohshiang Jong (Cambridge University, U.K.)
Martin Korth (University of Münster, Germany)
Martin Krupicka (Slovak Academy of Sciences, Bratislava, Slovakia)
Valentina Lacivita (University of Torino, Italy)
Robert Lee (Cambridge University, U.K.)
Pablo Lopez Rios (Cambridge University, U.K.)
Ryo Maezono (JAIST, Japan)
Mariapia Marchi (SISSA, Trieste, Italy)
Alston Misquitta (Cambridge University, U.K.)
Andrew Morris (Cambridge University, U.K.)

Richard Needs (Cambridge University, U.K.)
Norbert Nemec (Cambridge University, U.K.)
Priyanka Seth (Cambridge University, U.K.)
John Trail (JAIST, Japan)
Mike Towler (Cambridge University, U.K.)
Lucas Wagner (University of California, Berkeley, U.S.A.)
Ching-Ming Wei (Academia Sinica, Taiwan)
Shiwei Zhang (William and Mary College, U.S.A.)

### 3.1.2 Report on International Summer School "Quantum Monte Carlo and the CASINO program IV"

Sunday 2nd August - Sunday 9th August
The Apuan Alps Centre for Physics @ TTI, Vallico Sotto, Tuscany, Italy
`www.vallico.net/tti/tti.html`
Sponsors: Psi-k, CCP9
Organizer: Mike Towler
Conference web page: `www.vallico.net/tti/qmcatcp_09/summer_school.html`

The fourth international Quantum Monte Carlo Summer School took place at the Apuan Alps Centre for Physics in early August 2009 . The event was organized and run by Mike Towler, who was ably assisted with the teaching by Neil Drummond and Pablo López Ríos. All three instructors are members of the TCM Group from Cambridge University's Cavendish Laboratory. The purpose of the school was to provide the student with a thorough working knowledge of the quantum Monte Carlo electronic structure method as currently used in quantum chemistry and condensed matter physics, and to show him or her how to use the latest version of the Cambridge-developed QMC program CASINO for serious scientific research. The course consisted of around 20 hours of lectures and a series of practical exercises in using the CASINO program led by its authors. No previous background other than a basic knowledge of quantum mechanics was assumed, though it was stressed beforehand that a knowledge of density functional theory and similar methods is normally thought to be useful. As is usual at this venue, formal lectures were restricted to the mornings, and participants were given the freedom and space to think and to contemplate and discuss the issues at hand. In addition to hands-on exercises, a programme of healthy recreational activities such as mountain climbing was organized in the afternoons, during which the students were encourage to discuss their own research and to look into potential collaborations.

Quote from student: "*The summer school is an excellent in my whole life and I have really got inspired. I think every one who attends the QMC school will go back to home with great spirits. My words fail to explain how much I have enjoyed the lectures and outing trips. Thanks a lot for everything.. I will really miss you.*"

## Programme

The following lectures were given during the school:

**Mike Towler**

- Quantum Monte Carlo: a practical solution to the correlation problem in electronic structure calculations (2.5 hours)
- The CASINO program: a basic introduction to functionality and input/output (1 hour)
- Three QMC scaling problems (2 hours)
- Forces and dynamics. Expectation values other than the energy (2 hours)
- Practical aspects when using pseudopotentials with CASINO (1 hour)

**Pablo López Ríos**

- Statistical analysis for QMC (1 hour)
- Wave functions and nodes in QMC (2 hours)
- Pseudopotentials for QMC (1 hour)

**Neil Drummond**

- Diffusion Monte Carlo (2 hours)
- Optimization of many-electron wave functions (2 hours)
- Ewald interactions and finite size errors (2 hours)
- Some recent applications of quantum Monte Carlo simulation (1.5 hours)

During the afternoons the students completed the following exercises:

- Distribution, setup and compilation of the CASINO program
- Basic use of the CASINO program - simple VMC, DMC calculations
- Wave function optimization with CASINO
- Trial wave function generation with other programs (CRYSTAL/PWSCF/CASTEP etc.)
- Advanced use of the CASINO program (over two days)
- General CASINO applications

After the final lecture, a discussion session was held. Each student was asked to state their particular interest in the quantum Monte Carlo method; in each case the instructors attempted to give suitable advice for the chosen applications and to stimulate a short discussion.

The school was concluded with an exam in order to ascertain who had been paying attention. Just for the record, the student with the highest mark was James Shepherd of Cambridge University.

## List of participants

Twenty-five students from sixteen countries took part, accompanied by three family members, plus our nine staff. The names and institutions of the participants were:

Ariunbayasgalan Alyeksyei (Mongolian Academy of Sciences, Mongolia)
Mohaddeseh Abbasnejad (University of Tehran, Iran)
Grigor Aslanyan (University of California, San Diego, U.S.A.)
Alexandre Carvalho (University of Oporto, Portugal)
David Dell'Angelo (University of Rennes, France)
Andrea Droghetti (Trinity College, Dublin, Ireland)
Tim Green (University of Cambridge, U.K.)
Santosh KC (Tribhuvan University, Kathmandu, Nepal)
Duck Young Kim (University of Uppsala, Sweden)
Peter Larsson (University of Uppsala, Sweden)
Pablo Maldonado (University of Cordoba, Spain)
José Mira McWilliams (Universidad Politécnica de Madrid, Spain)
Miroslawa Nedyalkova (University of Sofia, Bulgaria)
Johan Pohl (University of Darmstadt, Germany)
José Roberto dos Santos Politi (University of Brasilia, Brazil)
Hannah Price (University of Cambridge, U.K.)
Narendra Revanuri (University of Goa, India)
Sergio Santos (University of Aveiro, Portugal)
Priyanka Seth (University of Cambridge, U.K.)
Vinit Sharma (Agrawal College, Jaipur, India)
James Shepherd (University of Cambridge, U.K.)
Stefano Spezia (University of Palermo, Italy)
Maria Velinova (University of Sofia, Bulgaria)
Márton Vörös (Budapest University, Hungary)
Arkadius Wojs (University of Cambridge, U.K.)

### 3.1.3 Report on the $14^{th}$ ETSF Workshop on Electronic Excitations: Ab-initio tools for the characterization of nanostructures

**Evora, Portugal**

**September 14-19, 2009**

**Sponsors: Psi-k, CECAM, ESF-SimBioMa, Fundação para a Ciência e Tecnologia**

**Fernando NOGUEIRA, Miguel Alexandre Lopes MARQUES, Ludger WIRTZ (local organizers)**
**Francesco SOTTILE, Valerio OLEVANO, Gian-Marco RIGNANESE, Patrick RINKE (program committee)**

**http://www.tddft.org/ETSF2009/index.html**

**Summary**

The workshop has focused on the first-principles description of electronic excitations and spectroscopy of condensed matter, nanostructures, and bio-molecules. In particular three methods for excited states calculations were addressed: i) Time-dependent density-functional theory (TDDFT), ii) Many-body perturbation theory (MBPT), i.e., the "GW-approximation" and the "Bethe-Salpeter Equation", iii) Quantum chemistry methods. We have discussed recent advances in both conceptual developments as well as their application to real systems. 95 researchers participated in the workshop. 5 keynote lectures, 8 invited talks, 26 contributed talks, and 30 posters were presented.

Tuesday, 15/09:
The first session on optical properties gave an overview over the use of advanced excited states methods (TDDFT, GW-approximation, Bethe-Salpeter Equation) in various systems. The opening keynote lecture by Steven Louie (UC Berkeley) dealt with the optical properties of graphene nanostructures and various possible device applications. Patrick Rinke (UC Santa Barbara) presented calculations of Auger recombination in nitrides, Hannes Hübener (Ecole Polytechnique, Paris) presented calculations of the second harmonic generation in Silicon. The session ended with two talks on novel materials for solar cells: Julien Vidal (Ecole Polytechnique, Paris) exposed how calculations beyond-DFT can help to improve the understanding of solar cells. Nicola Spallanzani (Modena) discussed photo-excitation in large organic molecules.

In the second keynote lecture, Gustavo Scuseria (Rice University) gave an overview over recent developments in hybrid functionals and on the mixing of the Random-Phase-Approximation with DFT.

In the session on bio-physics, different user projects of the ETSF were presented. Steen Nielsen

(Aarhus) gave a keynote lecture on how to perform measurements of absorption spectra of molecular ions in a storage ring experiment. Marius Wanko (San Sebastián) presented calculations in the QM/MM approach that accompany the experiment. Adriano Mosca Conte (Rome) presented results on the photo-excitation of proteins in the retina of the human eye.

Wednesday, 16/09:
The morning session was mainly devoted to strongly correlated systems. In a keynote lecture, Emily Carter (Princeton) introduced an approach to embed quantum-chemical wave-function methods into periodic DFT. One of the applications of this approach was the *ab-initio* description of the Kondo effect for transition metal impurities in nonmagnetic metallic hosts. Federico Iori and Matteo Guzzo (Ecole Polytechnique, Paris) reported on progress in the description of strongly correlated systems like $V_2O_3$ and NiO with a self-consistent GW-approach. Martin Stankovski (Louvain-la-Neuve) discussed the effects of self-consistency and semi-core states in the GW-approximation for Zn and Sn oxides. Jim Greer (Tyndall National Institute, Cork) presented a configuration-interaction method where the contributing (singly and multiply excited) configurations are chosen by a Monte Carlo approach. The session ended with a talk by Dietrich Foerster and Peter Koval (Bordeaux) on the extension of the LCAO method to excited states.

Walter Temmermann (Daresbury) presented a keynote lecture on the self-interaction-corrected local-spin-density (SIC-LSD) method for the calculation of rare earth and actinide compounds. In the following discussion it became clear that more work on the comparison of the different approaches for systems with strong localization and strong correlations should be tackled by the community in the future: self-consistent GW, SIC-LSD, and dynamical mean-field approximation (DMFT) have lead to enormous advances on different systems, but a detailed comparison of their performances is still missing.

The afternoon session was devoted to the random-phase approximation and functionals. Xinguo Ren (Fritz Haber Institute) assessed the potential of the random-phase approximation for CO adsorption and weakly bonded systems. Esa Räsänen (Jyväskylä, Finland) presented functionals in low-dimensional systems. Ulf von Barth (Lund) derived a correlation-energy functional from time-dependent exact-exchange theory.

Thursday, 17/09:
The first morning session dealt with the general theory for the description of quantum transport. Hervé Ness (York) presented a talk on non equilibrium and many-body effects in quantum transport through nanoscale devices. Hector Mera (CEA Grenoble) discussed the accuracy of conductances obtained from Kohn-Sham wave-functions. Valerio Olevano (Institut Néel, Grenoble) introduced a new quantum transport formalism based on a map of a real 3-dimensional system (lead-junction-lead) onto an effective 1-dimensional system and applied this approach to calculate the conductance through graphene nanoribbons. The second morning session was devoted to the transport properties of carbon nanostructures obtained at Louvain-la-Neuve (Belgium): Simon Dubois presented detailed calculations on the transport through graphene nanoribbons. Zeila Zanolli discussed transport properties of carbon atomic wires and Aurelien Lherbier showed the influence of dopants and defects on the transport in 2D graphene.

The afternoon session was devoted to recent developments of the GW-approximation. Juan María García Lastra (San Sebastián) demonstrated how to use the GW-approximation to cal-

culate image potentials at solid-molecule interfaces. Andreas Gierlich (Jülich) presented all-electron GW calculations for perovskite transition-metal oxides. Arjan Berger (Ecole Polytechnique, Paris) presented a scheme to calculate the GW self-energy without the use of unoccupied states. Pina Romaniello (Ecole Polytechnique, Paris) discussed the self-screening error of GW and the atomic limit of strong correlation within a two-site Hubbard model.

The subsequent poster session covered the whole range of electronic excitations from fundamental development of theory to its application to specific nano- and bio-systems.

Friday, 18/09:
Alberto Castro (Freie Universität Berlin) showed how to use TDDFT and optimal control theory to calculate the design of laser pulses that induce specific reactions in molecules (such as dissociation or isomerization). Ilya Tokatly (San Sebastián) discussed the continuum mechanics of quantum many-body systems in the linear response regime.

The following session dealt with optical properties of different materials: Andre Schleife (Jena) presented an application of the BSE-GW approach to the calculation of the optical spectra of MgO and ZnO in the presence of defects and doping. Marco Cazzaniga (Milano) showed RPA calculations of the electron-energy loss function of ferromagnetic iron. Giancarlo Cappellini presented a systematic TDDFT study of the optical spectra of polycyclic aromatic hydrocarbons. The session ended with a talk by Giovanni Onida (Milano) on the spectroscopy of monoatomic carbon wires.

In the afternoon, Pierluigi Cudazzo (San Sebastán) presented results towards an ab-initio description of high-temperature superconductivity in dense molecular hydrogen. Frank Fuchs (Jena) discussed the geometry, STM images and band structure of atomic gold-wires on a Ge(001) surface. Hans-Christian Weissker presented TDDFT calculations of the optical properties of silicon nanocrystals accompanied by molecular-dynamics simulations in order to elucidate the effect of temperature on the spectra.

## Program

| | | |
|---|---|---|
| | | **Sunday, September 13** |
| | | arrival day |
| 20:30 | | Dinner (at the Hotel - Buffet) |
| | | **Tuesday, September 15** |
| 9:00 | | Welcome address |
| 9:20 | *Steven Louie* | Spectroscopic and Transport Properties of Graphene and Graphene Nanostructures |
| 10:20 | | Coffee break |
| 10:50 | *Patrick Rinke* | Auger recombination rates in nitrides from first principles |
| 11:10 | *Hannes Huebener* | Second Harmonic Generation in Bulk Silicon |
| 11:30 | *Julien Vidal* | How can ab initio calculations help to improve solar cells? |
| 12:10 | *Nicola Spallanzani* | Photo-excitation of light-harvesting supra-molecular triad: a TDDFT study |
| 12:30 | | Lunch (at the Hotel) |
| 14:30 | *Gustavo Scuseria* | New models for mixing wavefunctions with density functional theory |
| 15:30 | | Coffee break |

| | | |
|---|---|---|
| 16:00 | *Steen Nielsen* | Absorption spectra of chromophore ions obtained from storage ring experiments |
| 17:00 | *Adriano Conte* | A theoretical investigation on the first step of the mechanism of vision in living beings |
| 17:20 | *Marius Wanko* | Multiscale Approaches for Protein Spectroscopy |
| 17:40 | | Round Table — Interaction of ETSF with users |
| 20:00 | | Dinner (at "Jardim do Pao" restaurant) |

**Wednesday, September 16**

| | | |
|---|---|---|
| 9:00 | *Emily Carter* | Ab Initio Treatment of Excited States and Strongly Correlated Electrons in Crystals |
| 10:00 | *Federico Iori* | In strong correlation do we trust? The paradigm of V2O3 |
| 10:20 | | Coffee break |
| 10:50 | *Matteo Guzzo* | Exchange and correlation effects in the electronic properties of transition-metal oxides: The example of NiO |
| 11:10 | *Martin Stankovski* | Oxidise this: A study of PAW+QPSCGW calculations on Zn and Sn oxides |
| 11:30 | *Jim Greer* | Calculation of electron correlations and excitation spectra from a Monte Carlo configuration generation technique |
| 12:10 | *Dietrich Foerster** | Extension of the LCAO method to excited states |
| 12:30 | | Lunch (at the Hotel) |
| 14:30 | *W. Temmermann* | Electronic and Magnetic Properties of Rare Earths and Actinide Compounds |
| 15:30 | | Coffee break |
| 16:00 | *Xinguo Ren* | Assessing the random phase approximation: CO adsorption and weakly bonded systems |
| 16:40 | *Esa Räsänen* | Functionals in low-dimensional systems |
| 17:00 | *Ulf von Barth* | Correlation energy functional and potential from time-dependent exact-exchange theory |
| 18:00 | | Cheese and wine tasting at "Rota dos Vinhos" |
| 20:00 | | Dinner (at "Adeguita do Farrobo" restaurant) |

* with Peter Koval

**Thursday, September 17**

| | | |
|---|---|---|
| 9:00 | *Hervé Ness* | Non equilibrium and many-body effects in quantum transport through nanoscale devices |
| 9:40 | *Hector Mera* | Are Kohn-Shamm conductances accurate? |
| 10:00 | *Valerio Olevano* | Effective 1D theory and generalized Fisher-Lee formula for quantum transport at nanocontacts |
| 10:20 | | Coffee break |
| 10:50 | *Simon Dubois* | Quantum Transport in Graphene Nanoribbons |
| 11:30 | *Zeila Zanolli* | Transport properties of carbon atomic wires |
| 11:50 | *Aurelien Lherbier* | Charge transport in 2D graphene including dopants/defects: ab initio and tight-binding coupled approach |
| 12:30 | | Lunch (at the Hotel) |
| 14:30 | *Juan Garcia-Lastra* | Classical and Many-Body Theory of Image Potentials at Solid-Molecule Interfaces |
| 15:10 | *Andreas Gierlich* | All-electron GW Calculations for Perovskite Transition-Metal Oxides |
| 15:30 | *J.A. Berger* | GW without empty states |
| 15:50 | *Pina Romaniello* | The self-energy beyond GW |
| 16:10 | | Coffee break |

| | | |
|---|---|---|
| 16:40 | | Poster Session |
| 20:00 | | Dinner (at "Jardim do Pao" restaurant) |

**Friday, September 18**

| | | |
|---|---|---|
| 9:00 | *Alberto Castro* | Quantum Optimal Control Theory with TDDFT |
| 9:40 | *Ilya Tokatly* | Linear Continuum Mechanics for Quantum Many-Body Systems |
| 10:00 | | Coffee break |
| 10:30 | *Andre Schleife* | From Ideal Bulk to Reality - Interplay of Excitonic Effects with Defects and Doping |
| 11:10 | *Claudia Roedl* | Absorption Spectra of Magn. Insulators: Antiferromagn. Trans.-Metal Oxides and Ferrogmagn. CrBr3 |
| 11:30 | *M. Cazzaniga* | Ab-initio long wavelength dielectric properties of bulk iron |
| 11:50 | *Giancarlo Cappellini* | Optical absorption ... polycyclic aromatic hydrocarbons |
| 12:10 | *Giovanni Onida* | Spectroscopy of Monoatomic Carbon wires connecting sp2 carbon fragments |
| 12:30 | | Lunch (at the Hotel) |
| 14:30 | *Pierluigi Cudazzo* | Ab Initio Description of High-Temperature Superconductivity in Dense Molecular Hydrogen |
| 14:50 | *Frank Fuchs* | Ab-initio study of atomic gold-wires on Ge(001) |
| 15:10 | *Hansi Weissker* | Temperature effects on the electronic and optical properties of silicon clusters |
| 15:30 | | Final remarks |
| 15:40 | | Coffee break |
| 16:00 | | ETSF Members' meeting |
| 20:00 | | Dinner (Banquet at the Hotel) |

**Saturday, September 19**

departure

## List of Posters:

| | |
|---|---|
| *Irene Aguilera* | First-Principles Design of Complex Intermediate-Band Photovoltaic Materials. |
| *Magdalena Birowska* | Ab initio study of functionalized carbon nanotubes |
| *Björn Oetzel* | Ab-Initio Studies of Electronic and Transport Properties of Graphene Nanoribbons |
| *Michel Bockstedte* | The merits of DFT-LDA and going beyond it towards excited states: a perspective from defects in SiC |
| *Duanjun Cai* | Accurate color tuning of firefly chromophore by modulation of local polarization electrostatic fields |
| *Fabiana Da Pieve* | Magnetic circular dichroism and spin polarization in resonant photoemission |
| *Louise Dash* | Non-equilibrium inelastic electronic transport: beyond the self-consistent Born approximation for the electron-phonon interaction |
| *Luiz Claudio de Carvalho* | First-Principles Study of the Structural and Electronic Properties of the (Al,Ga,In)N Compounds |
| *Xavier Declerck* | Electronic and transport properties of boron nitride nanoribbons |
| *Christoph Friedrich* | EXX within the full-potential augmented-planewave (FLAPW) method |
| *Pablo Garcia Gonzalez* | GW calculations in exactly solvable model systems: The problem of the self-interaction errors |
| *Matteo Gatti* | Excitonic effects in the absorption spectrum of sodium at high pressure |
| *Paola Gori* | Electronic and optical properties of group IV two-dimensional systems |
| *Jim Greer* | The ABC's of Many-Electron Correlated Scattering |

| | |
|---|---|
| *Ralf Hambach* | First-Principles Approach for Spatially-Resolved Electron Energy-Loss Spectroscopy |
| *Yann Pouillon* | Structural and optical transitions of biliverdin |
| *Fabrizio Puletti* | Large prebiotic molecules in space: photo-physics of acetic acid and its isomers |
| *Yuchen Ma* | excited states of the chromophores within many-body perturbation theory |
| *Anna Miglio* | Transparent Conducting Oxides (TCO): tin oxides as a case study |
| *Bruce Milne* | Time-Dependent DFT for Elucidation of Stereochemistry: Dermacozine E, a Natural Product from the Mariana Trench |
| *Bruce Milne* | FMO-TDDFT Studies of Luciferase from the Japanese Firefly Luciola cruciata |
| *Manolo Ramirez López* | Many carrier effects in semiconductor nanostructures |
| *Manolo Ramirez López* | Photoluminescence spectroscopy of InGaAs/GaAs quantum wells |
| *Tonatiuh RANGEL* | Transport properties of molecular junctions from Many-Body Perturbation Theory |
| *Arno Schindlmayr* | Do we know the band gap of lithium niobate? |
| *Martin Stankovski* | Oxidise this: A study of PAW + QPSC*GW* calculations on Zn and Sn oxides |
| *Z. Szotek* | Structural phase transitions and fundamental band gaps of $Mg_xZn_{1-x}O$ alloys from principles |
| *F. Trani* | Ab Initio simulation of photovoltaic materials |
| *José Guilherme Vilhena* | Density gradients for the exchange energy of electrons in two dimensions |
| *Ludger Wirtz* | The phonon dispersion relations of lead chalcogenides (PbS, PbSe, PbTe) |

**List of participants**

1. Steen Broendsted Nielsen
2. Andres R. Botello-Mendez
3. Alejandro Soba
4. Edgar Bea
5. Hector Mera
6. Marc Torrent
7. Davide Sangalli
8. Nicola Spallanzani
9. Fabrizio Puletti
10. Christoph Friedrich
11. Frank Fuchs
12. Luiz Claudio De Carvalho
13. Xinguo Ren
14. Andreas Gierlich
15. Ludger Wirtz
16. Roberto D'Agosta
17. Peter Koval
18. André Schleife
19. Björn Oetzel
20. Valerio Olevano
21. Paola Gori
22. Fabio Trani
23. Micael Oliveira
24. Miguel Marques
25. Arjan Berger

26. Christine Giorgetti
27. Eleonora Luppi
28. Federico Iori
29. Francesco Sottile
30. Gaelle Bruant
31. Hannes Huebener
32. Hans-Christian Weissker
33. Julien Vidal
34. Lucia Reining
35. Matteo Guzzo
36. Pina Romaniello
37. Ralf Hambach
38. Silvana Botti
39. Valerie Veniard
40. Ulf von Barth
41. Anna Miglio
42. Anne Matsuura
43. Aurélien Lherbier
44. Bruno Bertrand
45. Fabiana Da Pieve
46. Gian-Marco Rignanese
47. Jean-Cristophe Charlier
48. Martin Stankovski
49. Simon Dubois
50. Tonatiuh Rangel Gordillo
51. Xavier Declerck
52. Xavier Gonze
53. Zeila Zanolli
54. Emily A. Carter
55. Gustavo Scuseria
56. Dzidka Szotek
57. Walter Temmerman
58. Jim Greer
59. Carolina Roman
60. Ilya Tokatly
61. Juan María García Lastra
62. Marius Wanko
63. Matteo Gatti
64. Pierluigi Cudazzo
65. Xavier Andrade
66. Yann Pouillon
67. Pablo Garcia-Gonzalez
68. Irene Aguilera

69. Giovanni Onida
70. Marco Cazzaniga
71. Alberto Castro
72. Michel Bockstedte
73. Arno Schindlmayr
74. José Albuquerque D'orey
75. Dietrich Foerster
76. Giancarlo Cappellini
77. Patrick Rinke
78. Steven G. Louie
79. Bruce Milne
80. Claudia Cardoso
81. Duan-Jun Cai
82. Fernando Nogueira
83. Myrta Grüning
84. Tiago Cerqueira
85. Esa Räsänen
86. Yuchen Ma
87. Adriano Mosca Conte
88. Olivia Pulci
89. Karolina Milowska
90. Magdalena Birowska
91. Hervé Ness
92. James Ramsden
93. Louise Dash
94. Rex Godby
95. Tony Patman

### 3.1.4 Report on Workshop Computer Simulation of Oxides: Dopants, Defects and Surfaces

**Trinity College Dublin**

**9th - 11th September 2009**

**Science Foundation Ireland, Atlantic Centre for Atomistic Modelling, Psi-k Network and CECAM**

**Charles H. Patterson, School of Physics, Trinity College**

**Graeme Watson, School of Chemistry, Trinity College**

**Simon Elliott, Tyndall National Institute, Cork**

**Michael Nolan, Tyndall National Institute, Cork**

**www.tyndall.ie/research/theory-and-modelling/oxides-workshop/**

**www.cecam.org/workshop-347.html**

#### WORKSHOP SUMMARY

Computer simulation of oxides is a broad topic. This workshop had invited contributions on the role of oxides in catalysis, methods for electronic and atomic structures of oxides, defects and dopants in oxides and complex oxides such as cuprates. It consisted of 6 sessions under the headings: Surfaces and Catalysis, Electronic Structure Methods, Structure, Surfaces and Defects, Oxides and Dopants and Complex Oxides. It brought together around 70 researchers. There were ten invited speakers, 16 participants gave contributed talks and 24 posters were presented.

In the session on Surfaces and Catalysis, Horia Metiu (Santa Barbara) spoke on mechanisms of catalysed oxidation reactions investigated using density functional methods. Jörg Libuda (Erlangen) spoke on experimental spectroscopic studies of oxide storage catalysts aimed at improving the selectivity and activity of heterogeneous catalysts.

In the session on Electronic Structure Methods, Georg Kresse (Wien) spoke on application of hybrid functionals in the VASP code to oxygen vacancies in ZnO and formation of polarons in K doped $BaBiO_3$. He emphasised that these functionals predict lattice polarons in materials such as $BaBiO_3$, which conventional functionals do not. Hong Jiang (Beijing) spoke on application application of the GW approximation to lanthanide oxides beginning from an LDA+U state rather than a more conventional LDA state. In particular, he showed that GW calculations beginning from the LDA+U states give quantitative agreement with experimental band gaps of the series $Ln_2O_3$.

In the session on Structure, Alan Chadwick (Kent) gave an overview of application of X-ray absorption spectroscopy as a probe of structure of oxides, using microscopy and XAS to identify the surface morphology of oxide nanoparticles.

In the session on Surfaces and Defects, Richard Catlow (London) gave an overview of properties of ZnO predicted using DFT methods, including structure and properties of ZnO nano-particles, reactions catalysed at ZnO surfaces, and the structures of defects in ZnO. David Look (Ohio) gave an overview of optical spectroscopies of defects in ZnO formed by electron irradiation.

In the session on Oxides and Dopants, Su-Huai Wei (Colorado) covered properties of a wide range of oxides and their properties, including ZnO, $In_2O_3$, and $TiO_2$. Chris van de Walle (Santa Barbara) described recent work on calculating formation energies of defects in oxides. He described calculations of defect transition levels using conventional and hybrid density functional methods.

In the session on Complex Oxides, Francesc Illas (Barcelona) made a comparison between the electronic structures and exchange coupling constants in cuprate and pnictide superconductors and showed that the pnictides have a strongly frustrated interwoven network of exchange couplings between Fe ions.

One of the trends that has emerged in computer simulation of oxides is that hybrid density functionals such as the HSE functional give significantly improved predictions of oxide properties compared to density functionals which do not include Hartree-Fock exchange. These functionals are available in several codes and are now being fairly widely adopted for oxide simulation.

## WORKSHOP PROGRAMME

**9th September**

12:00 - 14:00 **Registration**
14:00 - 14:10 **Welcome**

**Surfaces and Catalysis**

14:10 15:00 **H. Metiu** Catalysis by Atomic Sized Centres
15:00 15:20 **J. Graciani** Cu, Au and Ce Nanoparticles Supported on $TiO_2$(110)
15:20 15:40 **G. Novell-Leruth** Selectivity in Oxidation Processes on $RuO_2$(110)

15:40 16:10 **Break**

16:10 17:00 **J. Libuda** Modelling Oxide Based Storage Catalysts
17:00 17:20 **R. Bennett** Non-Stoichiometric Titanium Dioxide: Experimental Insights and Challenges in Charge Transfer and Surface Reactions
17:20 17:40 **D. Costa** Realistic Ab Initio Model of the Passive Film Formed on Stainless Steels

17:40 18:00 **U. Wdowik** Lattice Dynamics of Co-Deficient and Fe-Doped CoO

18:00 20:00 **Poster Session and Reception**

**10th September**

**Electronic Structure Methods**

09:00 - 09:50 **G. Kresse** Hybrid Functionals and GW Applied to Simple and Complex Oxides
09:50 10:40 **H. Jiang** Localised and Itinerant States in $d$ and $f$ Electron Oxides united by $GW@LDA+U$
10:40 11:00 **H. Dixit** Quasiparticle Band Gap of IIB-VI Transparent Oxides within the GW Approximation

11:00 11:20 **Break**

**Structure**

11:20 12:10 **A. Chadwick** X-ray Absorption Spectroscopy: a Probe of Local Structure and Oxidation State
12:10 12:30 **K. P. McKenna** Electronic Properties of Defects in Polycrystalline Dielectric Materials
12:30 12:50 **R. Tétot** Multi Scale Modelling of Low Index Rutile $TiO_2$ Surfaces

12:50 15:00 **Lunch**

**Surfaces and Defects**

15:00 15:50 **R. Catlow** Modelling of Defects, Surface Properties and Nano Clusters of Zinc Oxide
15:50 16:10 **P. A. Mulheran** The Reduced Rutile (110) Surface: Energetics and Diffusion of Ti Point Defects in the Selvedge
16:10 16:30 **M. M. Islam** Electronic Properties of Oxygen Deficient and Metal Doped $TiO_2$

16:30 16:50 **Break**

16:50 17:40 **D. Look** Electrical and Optical Activity of Point Defects in ZnO
17:40 18:00 **S. Datta** Photoelectrolysis of Water for Hydrogen Production

19:30 **Dinner**

**11th September**

**Oxides and Dopants**

09:00 09:50 **S.-H. Wei** First-Principles Investigation of Unusual Materials Properties of Oxides
09:50 10:10 **A. Droghetti** Defect-Induced Magnetism in Oxides
10:10 10:30 **D. Scanlon** Intrinsic Ferromagnetism in $CeO_2$: Dispelling the Myth of Vacancy-Site-Localisation Mediated Superexchange

10:30 11:10 **Break**

11:10 12:00 **C. Van de Walle** Sources of Conductivity in Transparent Oxides
12:00 12:20 **A. Walsh** Band Alignment and Defect Physics of Functional Oxides

12:20 14:30 **Lunch**

**Complex Oxides**

14:30 15:20 **F. Illas** Similarities and Differences between Pnictides and Cuprate Superconducting Parent Compounds
15:20 15:40 **V. Fiorentini** Electronic Structure of Doped Cuprates by Self-Interaction-Corrected DFT
15:40 16:00 **P. Alippi** Role of Native Defects in the Dielectric and Conductivity Behaviour of $CaCu_3Ti_4O_{12}$

16:00 **Close**

## LIST OF POSTER TITLES AND FIRST AUTHORS

Titanocene Adsorption Studies on $TiO_2$(110) Rutile Surface Using Ab-Initio and Molecular Dynamics Approaches, **S. Agrawal**
Density Functional Theory of Doping in Both Bulk and Surface State Titania, Classical Simulation of $TiO_2$-Water Interface, **N. J. English**
Ab-Initio and Atomistic Simulation of Cu Doping in the Lead-Free Ferroelectric, **R. S. Kavathekar**
Perovskite Potassium Sodium Niobate, **S. Koerbel**
Small Polarons in Nb- and Ta-Doped Rutile and Anatase $TiO_2$, **B. J. Morgan**
Ferromagnetism in ZnO Induced by Complex Defects, **A. Chakrabarty**

Reconstruction of the Polar ZnO(0001) Surface, **H. Meskine**
Simulation of the Oxygen K edge Resonant X-ray Emission Spectroscopy of Rutile Titanium Dioxide, **C. McGuinness**
Energetics of Al Doping and Intrinsic Defects in Monoclinic and Cubic Zirconia: First Principles Calculations, **C. Århammar**
Self-Consistent First-Principles Method for Complex Disordered Materials, **A. Marmodoro**
Water Gas Shift Reaction on a Highly Active Inverse CeOx/Cu(111) Catalyst: Unique Role of Ceria Nanoparticles, **J. Graciani**
Transparent Conducting Oxides (TCO): Tin Oxides as a Case Study, **A. Miglio**
Origin of Ferromagnetism in Molybdenum Dioxide (MoO2) from Ab-Initio Calculation, **J. Nisar**
Simultaneous Multi-Parameter Scanning Probe Microscopy of $TiO_2$(110)-(1x1), **S. J. OBrien**
Competing Mechanisms in Atomic Layer Deposition of $La_2O_3$ versus $Er_2O_3$ from Cyclopentadienyl Precursors, **M. Nolan**
Role of the Substrate Surface on the Atomic Layer Deposition of Alumina on Silicon Nitride, **M. E. Grillo**
Correlation Effects in p-Electron Magnets: the case of $RbO_2$, **R. Kovacik**
Electronic Structure of Striped Phase of $Ca_{1.875}Na_{0.125}CuO_2Cl_2$, **C. H. Patterson**
Atomic Scale Modelling of Deposition Processes for High-k Dielectrics, **M. Shirazi and S. Klejna**
TCOs in the UV: a First-Principles Investigation of InOOH, $In(OH)_3$, $ZnO_2$, $Zn(OH)_2$, $CdO_2$, $Cd(OH)_2$, **M. P. Jigato**
Defects and Diffusion in $Cr_2O_3$: a DFT+U Study, **F. Lebreau**
Electronic Structure of Amorphous Silica using Extrapolar Method and PAW Formalism, **D. Waroquiers**
Defect States in Titanium Dioxide, **J. Stausholm-Möller**
Electronic Structure Calculations on the Oxygen Conductivity in $Ba_{0.5}Sr_{0.5}Co_{0.8}Fe_{0.2}O_3$, **M.-W. Lumey**

large**List of Participants**

Ms Saurabh Agrawal, University College Dublin, Ireland
saurabh.agarwal@ucdconnect.ie

Mr Jeremy Allen, Trinity College Dublin, Ireland
allenje@tcd.ie

Ms Paola Alippi, CNR-ISM, Italy
paola.alippi@ism.cnr.it

Dr Emilie Amzallag, CNRS-Univ. Paris Sud 11, France
emilie.amzallag@u-psud.fr

Ms Cecilia Århammar, RIT, Stockholm, Sweden
arhammar@kth.se

Dr Corrine Arrouvel, University of Bath, UK
C.Arrouvel@bath.ac.uk

Dr Roger Bennett, University of Reading, UK
r.a.bennett@reading.ac.uk

Mr Mario Burbano, Trinity College Dublin, Ireland
burbanom@tcd.ie

Mr Aurab Chakrabarty, Trinity College Dublin, Ireland
chakraa@tcd.ie

Prof. Richard Catlow, University College London, UK
c.r.a.catlow@ucl.ac.uk

Prof. Alan Chadwick, University of Kent, UK
A.V.Chadwick@kent.ac.uk

Mr Declan Cockburn, Trinity College Dublin, Ireland
cockburd@tcd.ie

Ms Dominique Costa, LPCS Chimie Paris Tech, France
dominique-costa@enscp.fr

Dr Soumendu Datta, Technical University of Denmark
sdatta@fysik.dtu.dk

Ms Hemant Dixit, University of Antwerp, Belgium
hemant.dixit@student.ua.ac.be

Mr Andrea Droghetti¡ Trinity College Dublin, Ireland
drogheta@tcd.ie

Dr Claude Ederer, Trinity College Dublin, Ireland
edererc@tcd.ie

Dr Simon Elliott, Tyndall National Institute, Ireland
simon.elliott@tyndall.ie

Dr Niall English, University College Dublin, Ireland
Niall.English@ucd.ie

Prof Vincenzo Fiorentini, Universita' di Cagliari, Italy
vincenzo.fiorentini@dsf.unica.it

Dr Daniel Fritsch, Trinity College Dublin, Ireland
fritschd@tcd.ie

Ms Natasha Galea, Trinity College Dublin, Ireland
galean@tcd.ie

Dr Jose RB Gomes, University of Aveiro, Portugal
jrgomes@ua.pt

Dr Jesus Graciani, University of Seville, Spain
graciani@us.es

Ms Maria-Elena Grillo, Tyndall National Institute, Ireland
Maria.grillo@tyndall.ie

Mr Morad El-Hendawy, University College Dublin, Ireland
Morad.elhendawy@ucd.ie

Dr Mohammad Mazharul Islam, Université P. et M. Curie, France
rana-islam@enscp.fr

Prof. Francesc Illas, University of Barcelona, Spain
francesc.illas@ub.edu

Dr Satoshi Itoh, Toshiba R and D Center, Japan
satoshi.itoh@toshiba.co.jp

Prof. Hong Jiang, Peking University, China
h.jiang@pku.edu.cn

Dr Maneul Perez Jigato, KU Leuven, Belgium
manuel.perezjigato@fys.kuleuven.be

Mr Ritwik Kavathekar, University College Dublin, Ireland
ritwik.kavathekar@ucdconnect.ie

Mr Patrick Keating, Trinity College Dublin, Ireland
keatinpr@tcd.ie

Mr Brian Kennedy, Trinity College Dublin, Ireland
bkennedy@tcd.ie

Ms Sylwia Klejna, Tyndall National Institute, Ireland
sylwia.klejna@gmail.com

Ms Sabine Koerbel, Fraunhofer IWM, Germany
sabine.koerbel@iwm.fraunhofer.de

Ms Kalle Korpela, Trinity College Dublin, Ireland
korpelak@tcd.ie

Dr Roman Kovacik, Trinity College Dublin, Ireland
kovacikr@tcd.ie

Prof. Georg Kresse
University of Vienna, Austria
Georg.kresse@univie.ac.at

Prof Joerg Libuda, University of Erlangen, Germany
Joerg.libuda@chemie.uni-relangen.de

Mr Francois Lebreau, ENSCP, France
francois-lebreau@enscp.fr

Prof. David Look, Wright State University, USA
David.Look@WPAFB.AF.MIL

Dr Marck Lumey, RWTH Aachen University, Germany
marck.lumey@ac.rwth-aachen.de

Mr Alberto Marmodoro University of Warwick, UK
a.marmodoro@warwick.ac.uk

Dr Cormac McGuinness, Trinity College Dublin, Ireland
Cormac.McGuinness@tcd.ie

Dr Keith McKenna, University College London, UK
k.mckenna@ucl.ac.uk

Dr Hakim Meskine, University of Strathclyde, UK
hakim.meskine@strath.ac.uk

Prof. Horia Metiu, Univ. California Santa Barbara, USA
metiu@chem.ucsb.edu

Ms Anna Miglio, Univ. Catholique de Louvain, Belgium
anna.miglio@uclouvain.be

Dr Benjamin Morgan, Trinity College Dublin, Ireland
benmorgan2@gmail.com

Dr Paul Mulheran, University of Strathclyde, UK
paul.mulheran@strath.ac.uk

Ms Jawad Nisar, Uppsala University, Sweden
jawad.nisar@fysik.uu.se

Dr Michael Nolan, Tyndall National Institute, Ireland
michael.nolan@tyndall.ie

Dr Gerard Novell-Leruth, Inst. Chem. Res. Catalonia, Spain
gnovell@iciq.es

Dr Simon O'Brien, Trinity College Dublin, Ireland
sjobrien@tcd.ie

Ms Marita O'Sullivan, Trinity College Dublin, Ireland
osullim6@tcd.ie

Dr Charles Patterson, Trinity College Dublin, Ireland
Charles.Patterson@tcd.ie

Dr Chaitanya Das Pemmaraju, Trinity College Dublin, Ireland
pemmaras@tcd.ie

Prof Stefano Sanvito, Trinity College Dublin, Ireland
sanvitos@tcd.ie

Mr David Scanlon, Trinity College Dublin, Ireland
scanloda@tcd.ie

Mr Mahdi Shirazi, Tyndall National Institute, Ireland
mahdi.shirazi@tyndall.ie

Mr Jess Stausholm-Møller, Aarhus University, Denmark
jsm@phys.au.dk

Dr Robert Tétot, CNRS-Univ. Paris Sud 11, France
robert.tetot@u-psud.fr

Prof. Chris van de Walle, Univ. California Santa Barbara, USA
vandewalle@mrl.ucsb.edu

Dr Aron Walsh, University College London, UK
aronjwalsh@gmail.com

Mr David Waroquiers, Univ. Catholique de Louvain, Belgium
david.waroquiers@uclouvain.be

Prof. Graeme Watson, Trinity College Dublin, Ireland
watsong@tcd.ie

Dr Urszula D. Wdowik, Pedagogical University, Cracow, Poland
sfwdowik@cyf-kr.edu.pl

Dr. Su-Huai Wei, NREL, USA
Suhuai.Wei@nrel.gov

### 3.1.5 Report on the CECAM workshop"Which electronic structure method for the study of defects?"

**EPF Lausanne, Switzerland, 8-10 June 2009**

## Description

The CECAM workshop "Which electronic structure method for the study of defects?" took place at CECAM headquarters in EPF Lausanne, Switzerland, 8-10 June 2009.

In terms of participation the workshop was one of the largest CECAM workshops in 2009, with almost 60 participants: besides 4 organizers (Prof. Jörg Neugebauer from MPIE Düsseldorf, Prof. Chris G. Van de Walle from University of California at Santa Barbara, Prof. Alfredo Pasquarello and Dr. Audrius Alkauskas from EPF Lausanne), there were 23 invited speakers, 27 people presenting posters, as well as 4 participants without a presentation. In terms of geography, 13 countries were covered: Austria, Belgium, Finland, France, Germany, Hungary, Ireland, Italy, Poland, Sweden, Switzerland, the UK, and the USA. Germany and the USA had the largest number of participants. The topic of the workshop was the theoretical study of point defects in solids. Recent decades have witnessed significant progress in electronic structure calculations based on density functional theory (DFT). When applied to defects, standard approximations to DFT largely fail because they suffer from the infamous band-gap problem. The latter consists of the severe underestimation of calculated bulk band gaps of semiconductors and insulators with respect to experiment. The band-gap problem hinders the direct comparison of calculated and measured defect formation energies and charge-transition levels, as well as the study of doping, etc. Furthermore, standard approximations also fail in cases where localization phenomena are important, such as in the description of polaronic effects or pseudo Jahn-Teller distortions. In recent years there has been an important development of methods which go beyond those standard approximations. These include the LDA+$U$ method, hybrid functionals, the $GW$ approximation, and others. These methods substantially relieve the band-gap problem, as well as the localization problem of standard density functionals.

The purpose of the workshop was to bring together scientists working in the development and application of these new methodologies. Since this is a fast-developing field, it was important to organize a workshop to see "what's what in the theory of defects". To give an example: different advanced methods can yield the experimental band gap but they nevertheless provide an incompatible description of defects. A possible reason is that one of the methods yields the correct band gap, but an erroneous band structure. Another possible reason is the incorrect description of the defect state in one of the competing theories. All of these factors eventually influence the reliability of achieved results. Equally significant, convergence studies of supercell calculations are extremely important and the presentation of not converged results is quite frequent in the field. This was also discussed in the workshop. More particularly, the topics of the workshop included: hybrid functionals (screened and bare) applied to defects, the $GW$

method and beyond, the LDA+$U$ method, supercell corrections, excited states of defects (the Bethe-Salpeter equation), quantum Monte-Carlo techniques, technical issues related to the use of hybrid functionals, calculations of systems with a large number of atoms, etc. There was a good combination of talks addressing specific issues and more general overview talks. Professor C. G. Van de Walle gave an introductory talk about the problem of first-principles defect calculations. Professor G. Scuseria reviewed the development in the field of hybrid functionals. It is clear that these will become more and more important with time. Professor W. R. L. Lambrecht provided a historical overview of the band-gap problem related to defect calculations. Professor J. Neugebauer presented his work on the calculation of the free energy of defects. The latter is often neglected in practical calculations but was shown to be important. Thus, in addition to its main focus which was on electronic structure theories and computational methodologies for the study of defects, the workshop turned out to be quite balanced, including a good mixture of theory, applications, insights, and overview.

The significance of theoretical calculations of defects is only going to grow in the future. To answer humanity's needs, such as those of energy, newer and more complex materials will be employed in technological applications. The performance of a certain material will be eventually determined not only by its electronic structure, but also by the control over its defects that will be achieved. As a result, experimental work will need more and more support from theory and simulations. We are thus confident that there will be more workshops and conferences devoted to this theme, and the present CECAM workshop was a very important contribution. The workshop was financially supported by CECAM and psi-k through MPIE Düsseldorf. More detailed information about the workshop, including abstracts of oral presentations and posters, can be found at http://www.cecam.org/workshop-291.html.

## List of participants

Audrius Alkauskas (EPFL, Switzerland)
Michel Bockstedte (Universität Erlangen-Nürnberg, Germany)
Patrick Briddon (University of Newcastle, UK)
Peter Broqvist (EPFL, Switzerland)
Christian Brouder (Université Pierre et Marie Curie, Paris, France)
Fabien Bruneval (CEA Saclay, France)
Alexandra Carvalho (EPFL, Switzerland)
James Chelikowsky (University of Texas at Austin, USA)
Stewart Clark (University of Durham, UK)
Fabiano Corsetti (Imperial College London, UK)
Jean-Paul Crocombette (SRMP, CEA Saclay, France)
Peter Deák (Bremen Center for Computational Materials Science, Germany)
Thierry Deutsch (CEA Grenoble, France)
Andrea Droghetti (Trinity College Dublin, Ireland)
Steven Erwin (Naval Research Laboratory, USA)
Francesco Filippone (CNR - Istituto di Struttura della Materia, Italy)
Christoph Freysoldt (MPI Düsseldorf, Germany)

Luigi Genovese (CEA Grenoble, France)
Luigi Giacomazzi (INFM Democritos and ICTP, Trieste, Italy)
Richard Hennig (Cornell University, USA)
Maria-Elena Grillo (Tyndall National Instittue, Ireland)
Ricardo Gomez Abal (Fritz-Haber-Institut der Max-Planck Gesellschaft, Germany)
Anderson Janotti (University of California Santa Barbara, USA)
ShinYoung Kang (Massachusetts Institute of Technology, USA)
Hannu-Pekka Komsa (Tampere University of Technology, Finland)
Deniz Kecik (Paul Scherrer Institut, Switzerland)
Piotr Kowalski (Ruhr Universität, Germany)
Georg Kresse (University of Vienna, Austria)
Dirk Lamoen (University of Antwerp, Belgium)
Walter R. L. Lambrecht (Case Western Reserve University, USA)
Björn Lange (MPI Dsseldorf, Germany)
Stephan Lany (National Renewable Energy Laboratory, Colorado, USA)
Layla Martin-Samos (CNR-INFM S3, Italy)
Blanka Magyari-Kope (Stanford University, USA)
Nikolaj Moll (IBM Research, Zürich Research Laboratory, Switzerland)
Jörg Neugebauer (Max-Planck Institute for Iron Research, Germany)
Joakim Nyman (Chalmers University of Technology, Sweden)
Gianfranco Pacchioni (Universitá Milano Bicocca, Italy)
Alfredo Pasquarello (EPFL, Switzerand)
Nicolas Richard (CEA-DAM-DIF, France)
Gian-Marco Rignanese (Catholic University of Leuven, Belgium)
Patrick Rinke (University of California at Santa Barbara, USA)
John Robertson (University of Cambridge, UK)
Michael Rohlfing (University of Osnabrück, Germany)
Guido Roma (SRMP/DMN/DEN CEA-Saclay, France)
Rolando Saniz (Universiteit Antwerpen, Belgium)
Kiroubanand Sankaran (IMEC - Université Catholique de Louvain, Belgium)
Gustavo Scuseria (Rice University, USA)
Ari Paavo Seitsonen (CNRS-IMPMC and Pierre and Marie Curie University, Paris 6, Finland)
Piotr Spiewak (Warsaw University of Technology, Poland)
Andras Stirling (Chem. Res. Cent., Budapest, Hungary)
Alexander Thiess (Jlich, Germany)
Paolo Umari (INFM Democritos, Trieste, Italy)
Joel Varley (University of California at Santa Barbara, USA)
Chris G. Van de Walle (University of California at Santa Barbara, USA)
David Waroquiers (Université Catholique de Louvain  PCPM, Belgium)
Su-Huai Wei (National Renewable Energy Laboratory, Colorado, USA)
Shengbai Zhang (Ransselaer Polytechnic Institute, USA)

## Programme

**Day 1 - Monday - June 8, 2009**

Morning session

* 08:45 to 09:00 - Registration
* 09:00 to 09:40 - Chris G. Van de Walle

    *Advances in Electronic Structure Methods for Defects and Impurities*
* 09:40 to 10:20 - James Chelikowsky

    *Quantum algorithms for modeling the properties of defects in nanocrystals and nanowires*
* 10:50 to 11:30 - Georg Kresse

    *Hybrid functionals and GW applied to complex materials*
* 11:30 to 12:10 - Anderson Janotti

    *LDA+U and hybrid functionals applied to the study of defects in oxide and nitride semiconductors*
* 12:10 to 12:50 - Gianfranco Pacchioni

    *Reduced and doped $TiO_2$: what is the nature of the defect states?*

Afternoon session

* 14:20 to 15:00 - Gustavo Scuseria

    *Progress on screened, multi- and local-range separated hybrids in DFT*
* 15:00 to 15:40 - Peter Deák

    *Accurate defect levels in Group IV semiconductors by the HSE06 functional in supercells*
* 16:10 to 16:50 - Audrius Alkauskas

    *"Band-gap problem" vs."band-edge problem" in theoretical calculations of defect energy levels*
* 16:50 to 17:30 - Patrick Briddon

    *Modelling thousands of atoms using Kohn-Sham density functional theory*
* 17:30 to 19:30 - Poster Session

**Day 2 - Tuesday - June 9, 2009**

Morning session

* 09:00 to 09:40 - John Robertson

    *Defect calculations using the screened exchange hybrid functional*
* 09:40 to 10:20 - Shengbai Zhang

    *Hybrid Functional Calculations of Jahn-Teller Defects*
* 10:50 to 11:30 - Peter Broqvist

    *Hybrid functional calculations of defects in high-k dielectrics and at semiconductor-oxide interfaces*
* 11:30 to 12:10 - Steven Erwin

    *Understanding doping in semiconductor nanocrystals*
* 12:10 to 12:50 - Su-Huai Wei

    *Overcoming the doping asymmetry problem in wide gap semiconductors*

Afternoon session

* 14:20 to 15:00 - Christoph Freysoldt

*Fully ab initio supercell corrections for charged defects*

* 15:00 to 15:40 - Stephan Lany

*Predicting p-orbital hole-polarons in DFT supercell calculations*

* 15:40 to 16:10 - Alfredo Pasquarello

*Hybrid-functional calculations with plane-wave basis sets: The effect of the integrable divergence on total energies, energy eigenvalues, and defect energy levels*

* 16:40 to 17:20 - Michael Rohlfing

*Excited states of defects in solids*

* 17:20 to 18:00 - Walter R. L. Lambrecht

*Unsolved problems with point defect calculations*

**Day 3 - Wedesday - June 9, 2009**

Morning session

* 09:00 to 09:40 - Jörg Neugebauer

*Computing free energy contributions of point defects*

* 09:40 to 10:20 - Richard Hennig

*Quantum Monte Carlo calculations for point defects in silicon*

*GW* session

* 10:50 to 11:30 - Michel Bockstedte

*The merits of DFT-LDA and beyond it towards excited states: a perspective from defects in SiC*

* 11:30 to 12:10 - Patrick Rinke

*Defect Formation Energies without the Band Gap Problem: Combining DFT and GW*

* 13:40 to 14:20 - Gian-Marco Rignanese

*A Many-Body Perturbation Theory perspective to defects in microelectronic devices and materials*

* 14:20 to 15:00 - Paolo Umari

*GW quasi-particle spectra from occupied states only*

* 15:00 to 15:40 - Layla Martin-Samos

*$SiO_2$ DFT and beyond*

* 15:40 to 16:20 - Ricardo Gomez Abal

*The f-electron challenge: localized and itinerant states in lanthanide oxides united by GW@LDA+U*

# 4 General Workshop/Conference Announcements

## 4.1 International Workshop on Quantum Monte Carlo in the Apuan Alps VI

**Apuan Alps Centre for Physics @ TTI**
**Vallico Sotto, Tuscany, Italy**

**Sat 24th - Sat 31st July 2010**

www.vallico.net/tti/tti.html

**A4 POSTER:**
www.tcm.phy.cam.ac.uk/∼mdt26/poster2.png

Continuing the series of alternative and very informal meetings at this venue, the Cambridge University Theory of Condensed Matter group is organizing a sixth International Workshop to discuss the development and application of the continuum quantum Monte Carlo method in condensed matter physics and quantum chemistry. The conference will take place in our 16th Century monastery in the mediaeval high mountain village of Vallico Sotto (in the Tuscan Apuan Alps near the beautiful Italian city of Lucca).

The normal format for these events involves formal presentations being restricted to the mornings, with the afternoons left free for relaxed discussion and participation in activities. For the young and vigorous, we organize mountain walks, caving and other healthy outdoor exercise, whilst the unfit and elderly might enjoy artistic tours, city visits, and gentle country strolls, with all participants reuniting in the evening for excellent Tuscan dinners in local restaurants. The monastery is a unique venue where the community spirit and magnificent location have inspired memorable meetings in the past.

This year's workshop will involve up to 35 people, all accommodated on site. Many speakers will be specifically invited, but anyone who feels that they have something to contribute and who wishes to attend the event is most welcome to contact the organizers (Mike Towler: mdt26 at cam.ac.uk) for further details. There is no charge either for attendance at the conference or accommodation.

FURTHER DETAILS/PHOTOGRAPHS/MATERIAL FROM PREVIOUS WORKSHOPS ACCESSIBLE ON TTI WEB PAGE - CLICK THE 'PUBLIC EVENTS' LINK.

TTI CURRENTLY TAKING BOOKINGS FOR THE HOSTING OF CONFERENCES, SCHOOLS AND GROUP MEETINGS IN EASTER/SUMMER 2010. Enquiries to mdt26 at cam.ac.uk .

### 4.2 Summer School on Quantum Monte Carlo and the CASINO program V

**Apuan Alps Centre for Physics @ TTI**
**Vallico Sotto, Tuscany, Italy**

**Sun 1st - Sun 8th August 2010**

`www.vallico.net/tti/tti.html`

**A4 POSTER:**
`www.tcm.phy.cam.ac.uk/~mdt26/poster.png`

The fifth international summer school in the series *Quantum Monte Carlo and the CASINO program* will take place during August 2010 at the TTI monastery in the Tuscan Apuan Alps in Italy, organized and hosted by members of Cambridge University physics department's Theory of Condensed Matter Group. The aim of the school is to give students a thorough introduction to quantum Monte Carlo as a method for performing high-quality calculations of the electronic structure of atoms, molecules, and materials. The course is designed for young quantum chemists or theoretical physicists who have no previous experience with this technique, though anyone interested is welcome to take part.

The monastery is a unique venue where the community spirit and magnificent location have inspired memorable workshops in the past. It is a delightful 16th century building incorporating an ancient church, and is situated in the isolated but spectacular setting of the Tuscan mountain village of Vallico Sotto. The church is fully equipped with relevant presentation and computer technology, and all accommodation is on-site. As with all events at the Institute, formal lectures are restricted to the mornings, and participants are given the freedom and space to think and to contemplate and discuss the issues at hand. In addition to hands-on exercises, a programme of healthy recreational activities will be organized in the afternoons, and it is hoped that by following this strict regime, together with breathing clean mountain air and by preparing and sampling fine Tuscan cuisine, the participant will be able to return home mentally and physically refreshed as well as better informed.

Describing the complex behaviour of materials at the atomic level requires a sophisticated description of the correlated motion of the electrons. Quantum Monte Carlo (QMC) is an increasingly popular and explicitly many-body method with the unusual capability of yielding highly accurate results whilst also exhibiting a very favourable scaling of computational cost with system size. Over the last eighteen years, the Cambridge group have been researching QMC methods and we have created a powerful, general computer program - CASINO - to carry out the calculations. The school will focus both on the basic theory of QMC and on more advanced practical techniques, and will include a thorough introduction to the CASINO program.

A background in density functional theory or similar - though not essential - is normally thought to be useful.

Instructors will include the main authors of the CASINO program (Dr. Mike Towler, Dr. Neil Drummond and Dr. Pablo Lopez Rios) and possibly others.

Participants would normally need to book a flight to Pisa airport from where onward transportation will be arranged (though other destinations are possible). Details of previous schools - including photographs - are available under the PUBLIC EVENTS link on the TTI web site.

Interested students should email Mike Towler (mdt26 at cam.ac.uk) for registration and further details.

# 5 Abstracts

## Ferromagnetism in Nitrogen-doped MgO: density-functional calculations

Phivos Mavropoulos, Marjana Ležaić, and Stefan Blügel
*Institut für Festkörperforschung (IFF)*
*and Institute for Advanced Simulation (IAS)*
*Forschungszentrum Jülich, D-52425 Jülich, Germany*

**Abstract**

The magnetic state of Nitrogen-doped MgO, with N substituting O at concentrations between 1% and the concentrated limit, is calculated with density-functional methods. The N atoms are found to be spin-polarized with a moment of 1 $\mu_B$ per Nitrogen atom and to interact ferromagnetically via the double exchange mechanism in the full concentration range. The long-range magnetic order is established above a finite concentration of about 1.5% when the percolation threshold is reached. The disorder is described within the coherent potential approximation, with the exchange interactions harvested by the method of infinitesimal rotations. The Curie temperature $T_{\rm C}$, calculated within the random phase approximation, increases linearly with the concentration, and is found to be about 30 K for 10% concentration. Besides the substitution of single Nitrogen atoms, also interstitial Nitrogen atoms, dimers and trimers and their structural relaxations are discussed with respect to the magnetic state. Possible scenarios of engineering a higher Curie temperature are analyzed, with the conclusion that an increase of $T_{\rm C}$ is difficult to achieve, requiring a particular attention to the choice of chemistry.

Accepted for publication in Phys. Rev. B.
Preprint: arXiv:0908.0934 [cond-mat.mtrl-sci]

# Quasiperiodic layers of free-electron metals studied using electron diffraction.

D' Souza[a], Sanjay Singh[a], D. Wu[b], T. A. Lograsso[b], M. Krajčí[c,d], J. Hafner[d], K. Horn[e], and S. R. Barman[a]

[a] *UGC-DAE Consortium for Scientific Research, Khandwa Road, Indore 452001, India*

[b] *Ames Laboratory, U.S. DOE, Iowa State University, Ames, IA 50011, USA*

[c] *Institute of Physics, Slovak Academy of Sciences, Dúbravská cesta 9, SK-84511 Bratislava, Slovak Republic*

[d] *Institut für Materialphysik and Center for Computational Materials Science, Universität Wien, Sensengasse 8/12, A-1090 Wien, Austria*

[e] *Fritz-Haber-Institut der Max-Planck-Gesellschaft, D-14195 Berlin, Germany*

**Abstract**

Using electron diffraction, we show that free-electron metals, such as sodium and potassium, form a highly regular quasiperiodic monolayer on the fivefold surface of icosahedral Al-Pd-Mn and that the quasiperiodicity propagates up to the second layer in sodium. Our photoelectron spectroscopy results show that the quasicrystalline alkali-metal adlayer does not exhibit a pseudogap near the Fermi level thought to be characteristic for the electronic structure of quasicrystalline materials. Calculations based on density functional theory provide a model structure for the quasicrystalline alkali-metal monolayer and confirm the absence of a pseudogap.

(Submitted to Phys. Rev. B **79** 134206 (2009) )

Contact person: fyzikraj@savba.sk

# Initial Pb adsorption on the five-fold Al-Pd-Mn quasicrystal surface

J. Ledieu[a], M. Krajčí[b,c], J. Hafner[b], L. Leung[d], L.H. Wearing[d], R. McGrath[d], T.A. Lograsso[e], D. Wu[e], V. Fournée[a]

[a] *LSG2M, CNRS UMR 7584, Ecole des Mines, Parc de Saurupt, 54042 Nancy Cedex, France*

[b] *Institut für Materialphysik and Center for Computational Materials Science, Universität Wien , Sensengasse 8/12, A-1090 Wien, Austria*

[c] *Institute of Physics, Slovak Academy of Sciences, Dúbravská cesta 9, SK-84511 Bratislava, Slovak Republic*

[d] *Surface Science Research Centre and Department of Physics, The University of Liverpool, Liverpool L69 3BX, UK*

[e] *Ames Laboratory, Iowa State University, Ames, IA 50011, USA*

**Abstract**

The initial adsorption of Pb on the five-fold Al-Pd-Mn quasicrystal surface has been investigated using scanning tunneling microscopy (STM) and *ab initio* calculations based on the density functional theory (DFT). In the sub-monolayer regime, Pb adsorbates are highly mobile and adsorb preferentially within the equatorially truncated pseudo-Mackay clusters present at the surface. The decoration of these unique adsorption sites leads to the formation of five-fold islands dubbed "starfish" and eventually to a quasiperiodic Pb monolayer. From the comparison of measured and calculated STM images it was concluded that most starfish clusters on all terraces are composed of ten Pb ad-atoms. The model of the structure of the starfish cluster has been proposed. The total energy calculations confirmed its stability. The experimentally observed characteristic features of the STM profile of the starfish cluster are also reproduced by the DFT calculations.

(Submitted to Phys. Rev. B **79** 165430 (2009) )

Contact person: fyzikraj@savba.sk

# Signatures of nonadiabatic $O_2$ dissociation at Al(111): First-principles fewest-switches study

Christian Carbogno[1], Jörg Behler[2], Karsten Reuter[3], Axel Groß[1]
[1]*Institut für Theoretische Chemie,*
*Universität Ulm, 89069 Ulm, Germany*
[2]*Lehrstuhl für Theoretische Chemie,*
*Ruhr-Universität Bochum, 44780 Bochum, Germany*
[3]*Fritz-Haber-Institut der Max-Planck-Gesellschaft,*
*Faradayweg 4–6, 14195 Berlin, Germany*

**Abstract**

Recently, spin selection rules have been invoked to explain the discrepancy between measured and calculated adsorption probabilities of molecular oxygen reacting with Al(111). In this work, we inspect the impact of nonadiabatic spin transitions on the dynamics of this system from first principles. For this purpose the motion on two distinct potential-energy surfaces associated to different spin configurations and possible transitions between them are inspected by means of the Fewest Switches algorithm. Within this framework we especially focus on the influence of such spin transitions on observables accessible to molecular beam experiments. On this basis we suggest experimental setups that can validate the occurrence of such transitions and discuss their feasibility.

(submitted to: Phys. Rev. B)
Contact person: Karsten Reuter (reuter@fhi-berlin.mpg.de)

# Doping of $C_{60}$-induced electronic states in BN nanopeapods

Vladimir Timoshevskii
*Department of Physics, McGill University, Montréal, Québec, Canada*

Michel Côté
*Département de physique et Regroupement Québécois sur les Matériaux de Pointe (RQMP),Université de Montréal, Montréal, Québec, Canada*

**Abstract**

We report the results of *ab initio* simulations of the electronic properties of a chain of $C_{60}$ molecules encapsulated in a boron nitride nanotube - so called BN-nanopeapod. It is demonstrated that this structure can be effectively doped by depositing potassium atoms on the external wall of the BN-nanotube. The resulting material becomes a true metallic one-dimensional crystal, where the conduction states are formed solely by the fullerene chain. At the doping rate of one K atom per $C_{60}$ molecule, the system shows the density of states at the Fermi level considerably higher than in any of the fullerene crystals presently made. This makes the doped BN-peapod structure an interesting candidate to study a possible superconducting state.

(Accepted for publication in Physical Review B, arXiv: 0911.0212)
Contact person: Michel Côté (Michel.Cote@umontreal.ca)

## Magnetically Hindered Chain Formation in Transition-Metal Break Junctions

Alexander Thiess, Yuriy Mokrousov, Stefan Heinze and Stefan Blügel
*Institut für Festkörperforschung and Institute for Advanced Simulation, Forschungszentrum Jülich, D-52425 Jülich, Germany and Institut für Theoretische Physik und Astrophysik, Christian-Albrechts-Universität zu Kiel, D-24098 Kiel, Germany*

**Abstract**

Based on first-principles calculations, we demonstrate that magnetism impedes the formation of long chains in break junctions. We find a distinct softening of the binding energy of atomic chains due to the creation of magnetic moments that crucially reduces the probability of successful chain formation. Thereby, we are able to explain the long standing puzzle why most of the transition metals do not assemble as long chains in break junctions and thus provide indirect evidence that in general suspended atomic chains in transition-metal break junctions are magnetic.

(Submitted to Physical Review Letters **103**, 217201 (2009))
Contact person: a.thiess@fz-juelich.de

## Orientation Dependence of the Intrinsic Anomalous Hall Effect in hcp Co

Eric Roman, Yuriy Mokrousov and Ivo Souza
*Department of Physics, University of California, Berkeley, California 94720, USA*

**Abstract**

We carry out first-principles calculations of the dependence of the intrinsic anomalous Hall conductivity of hcp Co on the spin magnetization direction. The Hall conductivity drops from 481 to 116 S/cm as the magnetization is tilted from the easy axis (c axis) to the ab plane. These values agree reasonably well with measurements on single crystals, while the angular average of 226 S/cm is in excellent agreement with the value of 205 S/cm measured in polycrystalline films. The strong intrinsic anisotropy is shown to arise from quasidegeneracies near the Fermi level.

(Submitted to Physical Review Letters **103**, 097203 (2009))
Contact person: y.mokrousov@fz-juelich.de

# Structurally driven magnetic state transition of biatomic Fe chains on Ir(001)

Yuriy Mokrousov, Alexander Thiess and Stefan Heinze
*Institut für Festkörperforschung and Institute for Advanced Simulation, Forschungszentrum Jülich, D-52425 Jülich, Germany*
*and Institut für Theoretische Physik und Astrophysik, Christian-Albrechts-Universität zu Kiel, D-24098 Kiel, Germany*
*and Institute of Applied Physics, University of Hamburg, D-20355 Hamburg, Germany*

**Abstract**

Using first-principles calculations, we demonstrate that the magnetic exchange interaction and the magnetocrystalline anisotropy of biatomic Fe chains grown in the trenches of the (51) reconstructed Ir(001) surface depend sensitively on the atomic arrangement of the Fe atoms. Two structural configurations have been considered which are suggested from recent experiments. They differ by the local symmetry and the spacing between the two strands of the biatomic Fe chain. Since both configurations are very close in total energy they may coexist in experiment. We have investigated collinear ferro- and antiferromagnetic solutions as well as a collinear state with two moments in one direction and one in the opposite direction (up-down-up-state). For the structure with a small interchain spacing, there is a strong exchange interaction between the strands and the ferromagnetic state is energetically favorable. In the structure with larger spacing, the two strands are magnetically nearly decoupled and exhibit antiferromagnetic order along the chain. In both cases, due to hybridization with the Ir substrate the exchange interaction along the chain axis is relatively small compared to free-standing biatomic iron chains. The easy magnetization axis of the Fe chains also switches with the structural configuration and is out-of-plane for the ferromagnetic chains with small spacing and along the chain axis for the antiferromagnetic chains with large spacing between the two strands. Calculated scanning tunneling microscopy images and spectra suggest the possibility to experimentally distinguish between the two structural and magnetic configurations.

(Submitted to Physical Review B **80**, 195420 (2009))
Contact person: y.mokrousov@fz-juelich.de

# Self-interaction corrected local spin density calculations of actinides

L. Petit[1,2], A. Svane[2], Z. Szotek[1], W.M. Temmerman[1], and G.M. Stocks[3]
*Daresbury Laboratory, Daresbury, Warrington WA4 4AD, United Kingdom*
*Department of Physics and Astronomy, Aarhus University,*
*DK-8000 Aarhus C, Denmark*
*Materials Science and Technology Division and Center for Defect Physics,*
*Oak Ridge National Laboratory, Oak Ridge, Tennessee 37831, USA*

**Abstract**

We use the self-interaction corrected local spin-density approximation in order to describe localization-delocalization phenomena in the strongly correlated actinide materials. Based on total energy considerations, the methodology enables us to predict the ground-state valency configuration of the actinide ions in these compounds from first principles. Here we review a number of applications, ranging from electronic structure calculations of actinide metals, nitrides and carbides to the behaviour under pressure of intermetallics, and O vacancies in $PuO_2$.

(To appear in the IOP Conference Series on Materials Science and Engineering )
Manuscript available from: leon.petit@stfc.ac.uk

# 6 Presenting Other Initiatives

## 6.1 First Official Release of the Exciting Code

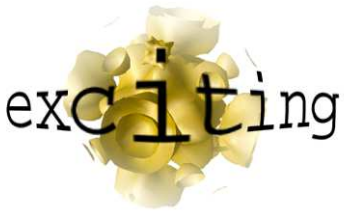


We would like to draw your attention to `exciting` *hydrogen*, the first official release of the exciting code. It is a full-potential all-electron density-functional-theory (DFT) package based on the linearized augmented planewave (LAPW) method. It can be applied to all kinds of materials, irrespective of the atomic species involved, and also allows for the investigation of the core region.

We particularly focus on excited state properties, within the framework of time-dependent DFT (TDDFT) as well as within many-body perturbation theory (MBPT).

`exciting` is developer-friendly through a clean and fully documented programming style, a modern source-code management, a dynamical build system, and automated tests. At the same time it is user-friendly, comprising various tools to create and validate input files and to analyze results.

Powerful packages are nourished from world-wide collaborations. Hence we are aiming at an open, transparent development process and encourage contributions from outside. Contact us if you want to join the developers team.

The code is available at `http://exciting-code.org`.

`exciting` has been recently introduced at the Graduate School in Bristol (Sept. 20 – 26, 2009). The hands-on tutorial *HoW* `exciting` will be held in November 2010 at the CECAM headquarter in Lausanne.

# 7 SCIENTIFIC HIGHLIGHT OF THE MONTH: "Electrical Polarization and Orbital Magnetization: The Modern Theories"

## Electrical Polarization and Orbital Magnetization: The Modern Theories

**Raffaele Resta**

Dipartimento di Fisica, Università di Trieste, Strada Costiera 11, I-34014 Trieste, Italy
and CNR-INFM DEMOCRITOS National Simulation Center, Trieste, Italy

**Abstract**

Macroscopic polarization **P** and magnetization **M** are the most fundamental concepts in any phenomenological description of condensed media. They are intensive vector quantities that intuitively carry the meaning of dipole per unit volume. But for many years both **P** and the orbital term in **M** evaded even a precise microscopic definition, and severely challenged quantum mechanical calculations. If one reasons in terms of a finite sample, the electric (magnetic) dipole is affected in an extensive way by charges (currents) at the sample boundary, due to the presence of the unbounded position operator in the dipole definitions. Therefore **P** and the orbital term in **M**—phenomenologically known as a bulk properties—apparently behave as surface properties; only spin magnetization is problemless. The field has undergone a genuine revolution since the early 1990s. Contrary to a widespread incorrect belief, **P** *has nothing to do* with the periodic charge distribution of the polarized crystal: the former is essentially a property of the *phase* of the electronic wavefunction, while the latter is a property of its *modulus*. Analogously, the orbital term in **M** has nothing to do with the periodic current distribution in the magnetized crystal. The modern theory of polarization, based on a Berry phase, started in the early 1990s and is now implemented in most first-principle electronic structure codes. The analogous theory for orbital magnetization started in 2005 and is partly work in progress. In the electrical case calculations have concerned various phenomena (ferroelectricity, piezoelectricity, and lattice dynamics) in several materials, and are in spectacular agreement with experiments; they have provided thorough understanding of the behavior of ferroelectric and piezoelectric materials. In the magnetic case the very first calculations are appearing at the time of writing (2009). Here I review both theories on an uniform ground in a DFT framework, pointing out analogies and differences. Both theories are deeply rooted in geometrical concepts, elucidated in this work. The main formulas for crystalline systems express **P** and **M** in terms of Brillouin-zone integrals, discretized for numerical implementation. I also provide the corresponding formulas for disordered systems in a single **k**-point supercell framework. In the case of **P** the single point formula has been widely used in the Car-Parrinello community to evaluate IR spectra.

# 1 Introduction

Polarization **P** and magnetization **M** are fundamental concepts that all undergraduates learn about in elementary courses [1, 2]. In view of this, it is truly extraordinary that until rather recently there was no generally accepted formula for both electrical polarization and orbital magnetization in condensed matter, even as a matter of principles. Computations of both **P** and **M** for real materials were therefore impossible. It is important to stress that we are addressing here "polarization itself" and "magnetization itself", while instead linear-response theory has satisfactorily provided **P** derivatives over the years and, more recently, even **M** derivatives.

In the case of **P**, a genuine change of paradigm was initiated by a couple of important papers [3,4], after which the major development was introduced by King-Smith and Vanderbilt in 1992 (paper published in 1993 [5]). Other important advances continued during the 1990s [6, 7] and the so-called "modern theory of polarization" is at a mature stage since about a decade. Among other things, the modern theory shed new light on previous linear-response formulations. Several reviews have appeared in the literature: the very first one is Ref. [8] and the most recent ones are Refs. [9, 10].

In the case of **M** (or, more precisely, of the *orbital contribution* to **M**) a similar breakthrough only occurred in 2005 [11, 12], and the "modern theory of magnetization" is partly work in progress.

Aiming at the $\Psi_{\mathbf{k}}$ community, it is worth emphasizing that most ab-initio electronic-structure codes on the market, for dealing with either crystalline or noncrystalline materials, implement the modern theory of polarization as a standard option. A nonexaustive list includes ABINIT [13], CPMD [14] CRYSTAL [15], QUANTUM-ESPRESSO [16], SIESTA [17], and VASP [18]. Implementations of the modern theory have been instrumental since more than a decade in the study of ferroelectric and piezoelectric materials [19–21]. The basic concepts of the modern theory of polarization also start reaching a few textbooks, though very slowly; most of them are still plagued with erroneous concepts and statements.

At variance with the electrical case, the modern theory of magnetization is still in its infancy. Key developments are in progress [22–26], and first-principle calculations just start appearing [27,28]. A CECAM workshop centered on the latest developments, and partly supported by $\Psi_{\mathbf{k}}$, was organized in June 2009 [29].

Macroscopic polarization may only occur in absence of inversion symmetry, while macroscopic magnetization requires absence of time-reversal symmetry. Another key difference is that polarization (as a bulk material property) only makes sense in insulating materials, while macroscopic magnetization exists both in insulators and metals. A material is insulating, in principle, only at $T = 0$, hence the modern theory of polarization is intrinsically a $T = 0$ theory. At variance with this, the modern theory of magnetization can be extended to $T \neq 0$ [23, 24].

Macroscopic polarization is the sum of two contributions: electronic and nuclear. Only the first term requires quantum-mechanical treatment, but it is mandatory to consider the two terms altogether, since overall charge neutrality is essential.

Macroscopic magnetization is a purely electronic phenomenon, but it is the sum of two con-

tributions as well: spin magnetization and orbital magnetization. The latter occurs whenever time-reversal symmetry is broken in the spatial wavefunction. For instance, in a ferromagnet the spin-orbit interaction transmits the symmetry breaking from the spin degrees of freedom to the spatial (orbital) ones; the two contributions to the total magnetization can be resolved experimentally. Other examples include systems in *applied* magnetic fields. Whenever the unperturbed system is nonmagnetic and insulating, the induced magnetization is 100% of the orbital kind.

The modern theory of magnetization also allows the computation of NMR shielding tensors in condensed matter [27], in an alternative way with respect to the linear-response approach (in the long-wavelength limit) currently used since more than a decade by Mauri and coworkers [30].

# 2 Macroscopics

## 2.1 Fundamentals

The basic microscopic quantities inside a material are the local microscopic fields $\mathbf{E}^{(\mathrm{micro})}(\mathbf{r})$ and $\mathbf{B}^{(\mathrm{micro})}(\mathbf{r})$, which fluctuate at the atomic scale. By definition, the macroscopic fields $\mathbf{E}$ and $\mathbf{B}$ are obtained by averaging them over a macroscopic length scale [2]. In a macroscopically homogeneous system the macroscopic fields $\mathbf{E}$ and $\mathbf{B}$ are constant, and in crystalline materials they coincide with the cell average of $\mathbf{E}^{(\mathrm{micro})}(\mathbf{r})$ and $\mathbf{B}^{(\mathrm{micro})}(\mathbf{r})$.

The constituent equations of electrostatics and magnetostatics in continuous media are, to linear order in the fields [1]

$$\mathbf{D} = \mathbf{E} + 4\pi\mathbf{P}; \qquad \mathbf{B} = \mathbf{H} + 4\pi\mathbf{M}, \tag{1}$$

where $\mathbf{P}$ and $\mathbf{M}$ are the macroscopic polarization and magnetization, respectively. All macroscopic quantities entering Eq. (1) may have a spatial dependence only at inhomogenous regions, where a net electrical charge density $\rho(\mathbf{r})$ and/or a dissipationless current density $\mathbf{j}(\mathbf{r})$ pile up according to

$$\nabla \cdot \mathbf{P}(\mathbf{r}) = -\rho(\mathbf{r}); \qquad \nabla \times \mathbf{M}(\mathbf{r}) = \frac{1}{c}\mathbf{j}(\mathbf{r}). \tag{2}$$

At an interface between two different homogeneous media $\mathbf{P}$ and $\mathbf{M}$ are in general discontinuous.

In the simple case of the surface of an homogenously polarized and/or magnetized medium, $\mathbf{P}$ and $\mathbf{M}$ vanish on the vacuum side. Eq. (2) implies the occurrence of a surface charge and/or a surface current

$$\sigma_{\mathrm{surface}} = \mathbf{P} \cdot \mathbf{n}, \qquad \mathbf{K}_{\mathrm{surface}} = c\,\mathbf{M} \times \mathbf{n}, \tag{3}$$

where $\mathbf{n}$ is the normal to the surface. Notice that $\mathbf{M}$ is a well defined quantity for either insulating or metallic materials; instead $\mathbf{P}$ is a nontrivial, material dependent, property only in insulating materials. In the metallic case $\sigma_{\mathrm{surface}}$ completely screens any electrical perturbation (Faraday-cage effect), hence $\mathbf{P}$ is trivial and universal.

We transform Eq. (1) using the dielectric and magnetic permeability tensors

$$\overleftrightarrow{\varepsilon} = \frac{\partial \mathbf{D}}{\partial \mathbf{E}}; \quad \overleftrightarrow{\mu} = \frac{\partial \mathbf{B}}{\partial \mathbf{H}}, \tag{4}$$

$$\mathbf{P} = \mathbf{P}_0 + \frac{\overleftrightarrow{\varepsilon} - 1}{4\pi}\mathbf{E}; \qquad \mathbf{M} = \mathbf{M}_0 + \frac{\overleftrightarrow{\mu} - 1}{4\pi}\mathbf{H}. \tag{5}$$

Because of symmetry reasons, the polarization $\mathbf{P}_0$ in a null $\mathbf{E}$ field can be nonzero only if the unperturbed medium breaks inversion symmetry; analogously, the magnetization $\mathbf{M}_0$ in a null $\mathbf{B}$ field can be nonzero only if the unperturbed medium breaks time-reversal symmetry.

The modern theory of polarization, at least in its original form, only addresses $\mathbf{P}_0$, the polarization *in a null field*, also known (for reasons explained below) as the "transverse" polarization. Quite analogously the modern theory of orbital magnetization, at the present stage of development, only addresses $\mathbf{M}_0$, the magnetization in a null field.

In condensed matter theory one addresses bulk quantities, with no reference to real finite samples with boundaries. The microscopic fields $\mathbf{E}^{(\mathrm{micro})}(\mathbf{r})$ and $\mathbf{B}^{(\mathrm{micro})}(\mathbf{r})$ are ideally measurable inside the materal, with no reference to what happens outside a finite sample. Their macroscopic averages $\mathbf{E}$ and $\mathbf{B}$, i.e. the internal (or screened) macroscopic fields, are therefore the variables of choice for a first-principle description. It must be realized that, insofar as we address an infinite system with no boundaries, the macroscopic field (either $\mathbf{E}$ or $\mathbf{B}$) is just an arbitrary boundary condition. To realize this, it is enough to focus on the electrical case for a crystalline material. The microscopic charge density is neutral in average and lattice periodical; the value of $\mathbf{E}$ is just an arbitrary boundary condition for the integration of Poisson's equation. The usual choice (performed within all electronic-structure codes) is to impose a lattice-periodical Coulomb potential, i.e. $\mathbf{E} = 0$. Imposing a given nonzero value of $\mathbf{E}$ is equally legitimate (in insulators), although technically more difficult [31, 32]).

In order to study the bulk material properties of a macroscopically homogeneous system it is quite convenient to address the infinite system with no boundaries. The above formulation of electrostatics and magnetostatics is sufficient and ideally suited for electronic structure theory: there is no need of addressing external (or unscreened) fields, as there is no need of addressing the auxiliary and unphysical fields $\mathbf{D}$ and $\mathbf{H}$.

For instance, the dielectric tensor $\overleftrightarrow{\varepsilon}$ defined by Eq. (4) is best addressed within electronic structure theory as

$$\overleftrightarrow{\varepsilon} = 1 + 4\pi \frac{\partial \mathbf{P}}{\partial \mathbf{E}}, \tag{6}$$

where only "internal" quantities (well defined in the bulk of the sample), and no "external" ones, appear. Obviously, for a homogeneous material, $\overleftrightarrow{\varepsilon}$ is a bulk material property, independent of the sample shape.

There are actually *two* different dielectric tensors: the genuinely static one, called $\overleftrightarrow{\varepsilon}_0$, and the so-called "static high frequency", called $\overleftrightarrow{\varepsilon}_\infty$. The latter accounts for the electronic polarization only, and is also called "clamped-ion" dielectric tensor. Both are experimentally measurable [33].

## 2.2 Finite samples and shape issues

Even if there is no need of addressing finite samples and external vs internal fields from a theoretician's viewpoint, such a digression can be quite instructive given that experiments *are* performed over finite samples, often in external fields.

We start with the electrical case. Suppose a finite macroscopic sample is inserted in a constant external field $\mathbf{E}^{(\mathrm{ext})}$: the microscopic field $\mathbf{E}^{(\mathrm{micro})}(\mathbf{r})$ coincides with $\mathbf{E}^{(\mathrm{ext})}$ far away from the

sample, while it is different inside because of screening effects. If we choose an homogeneous sample of *ellipsoidal shape*, then the macroscopic average of $\mathbf{E}^{(\mathrm{micro})}(\mathbf{r})$, i.e. the macroscopic screened field $\mathbf{E}$, is constant in the bulk of the sample.

The shape effects are embedded in the depolarization coefficients $n_\alpha$, defined in Ref. [1], with $\sum_\alpha n_\alpha = 1$; Greek subscripts indicate Cartesian coordinates throughout. Special cases are the sphere ($n_x = n_y = n_z = 1/3$), the extremely prolate ellipsoid, i.e. a cylinder along $z$ ($n_x = n_y = 1/2, n_z = 0$), and the extremely oblate one, i.e. a slab normal to $z$ ($n_x = n_y = 0, n_z = 1$).

The main relationship between $\mathbf{E}$, $\mathbf{E}^{(\mathrm{ext})}$, and $\mathbf{P}$ is [1]:

$$E_\alpha = E_\alpha^{(\mathrm{ext})} - 4\pi n_\alpha P_\alpha. \tag{7}$$

When we consider a free-standing finite system, with *no* external field, Eq. (7) provides by definition the depolarizing field. In the simple case of a slab geometry the depolarizing field is $\mathbf{E} = -4\pi\mathbf{P}$ when $\mathbf{P}$ is normal to the slab, and $\mathbf{E} = 0$ when $\mathbf{P}$ is parallel to the slab: this is sketched in Fig. 1.

Quite generally, a vector field is called "longitudinal" when it is curl-free, and "transverse" when it is divergence-free: we analyze $\mathbf{P}(\mathbf{r})$ and $\mathbf{M}(\mathbf{r})$ as functions of a macroscopic coordinate across the slab in this respect. The external fields are set to zero.

When $\mathbf{P}(\mathbf{r})$ it is normal to the slab we have $P_z = P_z(z)$ (indipendent of $xy$): hence at the slab boundary $\nabla \cdot \mathbf{P} \neq 0$, $\nabla \times \mathbf{P} = 0$: the normal polarization is longitudinal. When $\mathbf{P}(\mathbf{r})$ is parallel to the slab we have $P_x = P_x(z)$ (independent of $xy$): hence at the boundary $\nabla \cdot \mathbf{P} = 0$, $\nabla \times \mathbf{P} \neq 0$: the parallel polarization is transverse (see Fig. 1). Looking at Eq. (5), it is clear that the transverse polarization coincides with $\mathbf{P}_0$, while (for isotropic permittivity) the longitudinal one is $\mathbf{P} = \mathbf{P}_0/\varepsilon$. These are the extreme values; for an arbitrary ellipsoidal shape $\mathbf{P}$ will be intermediate between them.

A subtle issue is: which $\varepsilon$ is to be used? $\varepsilon_0$ or $\varepsilon_\infty$? The answer is always $\varepsilon_0$, with the only notable exception of lattice dynamics. If $\mathbf{P}_0$ is the polarization of a given "frozen phonon" at zero field (i.e. transverse), the corresponding longitudinal polarization (for the same displacements pattern) is $\mathbf{P} = \mathbf{P}_0/\varepsilon_\infty$. This follows immediately e.g. from Huang's phenomenological theory [34, 35].

Next, we switch to the magnetic case. Again, by definition, the magnetization normal to the

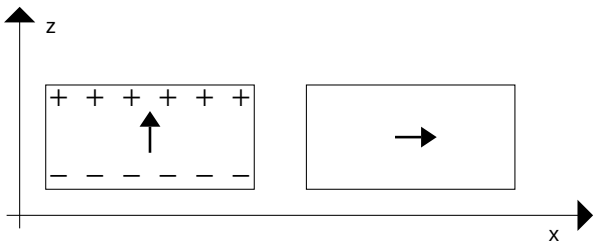


Figure 1: Electrical macroscopic polarization $\mathbf{P}$ in a slab normal to $z$, for a vanishing external field $\mathbf{E}^{(\mathrm{ext})}$. Left: When $\mathbf{P}$ is normal to the slab, a depolarizing field $\mathbf{E} = -4\pi\mathbf{P}$ is present inside the slab, and charges at its surface, with areal density $\sigma_{\mathrm{surface}} = \mathbf{P} \cdot \mathbf{n}$ Right: When $\mathbf{P}$ is parallel to the slab, no depolarizing field and no surface charge is present.

slab is longitudinal and the parallel one is transverse. According to Ref. [1], one has to replace $\mathbf{P}$ with $\mathbf{M}$, $\mathbf{E}$ with $\mathbf{H}$, and $\mathbf{E}^{(\mathrm{ext})}$ with $\mathbf{H}^{(\mathrm{ext})} = \mathbf{B}^{(\mathrm{ext})}$. The analogue of Eq. (7) is then

$$H_\alpha = B_\alpha^{(\mathrm{ext})} - 4\pi n_\alpha M_\alpha. \tag{8}$$

We eliminate $\mathbf{H}$ by means of Eq. (1); then for a uniformly magnetized ellipsoid in zero external field $\mathbf{B}^{(\mathrm{ext})}$ the demagnetizing field is

$$B_\alpha = 4\pi(1 - n_\alpha)M_\alpha. \tag{9}$$

We consider once more the slab geometry, in which case $\mathbf{B} = 4\pi\mathbf{M}$ when $\mathbf{M}$ is parallel to the slab, and $\mathbf{B} = 0$ when $\mathbf{M}$ is normal to the slab: this is sketched in Fig. 2. In the case of isotropic permeability Eqs. (4) and (5) lead to

$$\mathbf{M} = \mathbf{M}_0 + \frac{\mu - 1}{4\pi\mu}\mathbf{B}, \tag{10}$$

It follows immediately that $\mathbf{M} = \mathbf{M}_0$ when the magnetization is normal to the slab (longitudinal), while it is easily verified that $\mathbf{M} = \mu\mathbf{M}_0$ when the magnetization is parallel (transverse). In analogy to the electrical case, these are the extreme values; for an arbitrary ellipsoidal shape $\mathbf{M}$ will be intermediate between them.

It is customary to write $\mu = 1 + 4\pi\chi$, where $\chi$ is the magnetic susceptibility. This can be positive or negative, but is fairly small with the notable exception of ferromagnetic materials in a neighborhood of the phase transition [1]. In most cases we can expand Eq. (10) as

$$M_\alpha \simeq M_{0,\alpha} + \chi B_\alpha = M_{0,\alpha} + 4\pi\chi(1 - n_\alpha)M_\alpha. \tag{11}$$

For a spherical sample ($n_\alpha = 1/3$) the leading-order shape correction is

$$\mathbf{M} \simeq \left(1 + \frac{8\pi}{3}\chi\right)\mathbf{M}_0. \tag{12}$$

Finally, we summarize the slab results end we emphasize the key difference when the slab is in zero external fields. In the electrical case the *transverse* (i.e. parallel to the slab) polarization $\mathbf{P} = \mathbf{P}_0$ occurs in zero $\mathbf{E}$ (internal) field, while in the magnetic case it is the *longitudinal* (i.e. normal to the slab) magnetization $\mathbf{M} = \mathbf{M}_0$ which occurs in zero $\mathbf{B}$ (internal) field. This is confirmed by absence of surface charges and surface currents in these geometries (see Figs. 1 and 2).

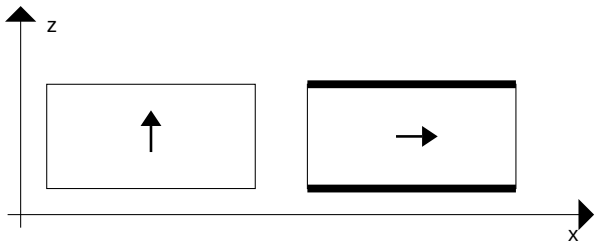


Figure 2: Macroscopic magnetization $\mathbf{M}$ in a slab normal to $z$, for a vanishing external field $\mathbf{B}^{(\mathrm{ext})}$. Left: When $\mathbf{M}$ is normal to the slab, no depolarizing field and no surface current is present. Right: When $\mathbf{M}$ is parallel to the slab, a demagnetizing field $\mathbf{B} = 4\pi\mathbf{M}$ is present inside the slab, and dissipationless currents $\mathbf{K}_{\mathrm{surface}} = c\,\mathbf{M} \times \mathbf{n}$ flow at the surfaces.

# 3 Microscopics

Intuitively, the macroscopic polarization $\mathbf{P}$ and magnetization $\mathbf{M}$ should be intensive vector properties carrying the meaning of electric/magnetic dipole per unit volume. Most texbooks attempt at a microscopic definition of $\mathbf{P}$ in a crystal in terms of the dipole moment per cell [33,36], but such approaches are deeply flawed because there is no unique choice for the cell boundaries [37].

In the magnetic case there is an outstanding difference between spin and orbital contributions to $\mathbf{M}$. The two contributions are unambiguously defined in nonrelativistic (and semirelativistic) quantum mechanics, and can be experimentally resolved in several cases. The spin contribution is very simple: the microscopic spin density is a well defined quantity, and can be interpreted as a "dipolar density". In the crystalline case, the spin contribution to $\mathbf{M}$ is then proportional to the cell-averaged spin density. At variance with this, the orbital contribution to $\mathbf{M}$ suffers of the same problems as $\mathbf{P}$. In the following, we are not going to address spin magnetization anymore, and we are using the symbol $\mathbf{M}$ to indicate the orbital term only.

Given the intuitive meaning of $\mathbf{P}$ and $\mathbf{M}$, it is tempting to define them as the dipole moment of a sample, divided by the volume $V$:

$$\mathbf{P} = \frac{\mathbf{d}}{V} = \frac{1}{V}\int d\mathbf{r}\ \mathbf{r}\rho^{(micro)}(\mathbf{r}), \qquad \mathbf{M} = \frac{\mathbf{m}}{V} = \frac{1}{2cV}\int d\mathbf{r}\ \mathbf{r}\times\mathbf{j}^{(micro)}(\mathbf{r}),, \tag{13}$$

where $\rho^{(micro)}(\mathbf{r})$ and $\mathbf{j}^{(micro)}(\mathbf{r})$ are the microscopic charge and current densities. Notice that there is no such thing as a "dipolar density": the basic microscopic quantities are $\rho^{(micro)}(\mathbf{r})$ and $\mathbf{j}^{(micro)}(\mathbf{r})$. If the sample is *uniformly* polarized/magnetized, then the microscopic charge/current averages to zero in the bulk of the sample, while at the sample boundary a net charge piles up and/or a dissipationless current flows, in agreement with the macroscopic Eq. (3). Phenomenologically $\mathbf{P}$ and $\mathbf{M}$ are *bulk* material properties, while from the above considerations they apparently are *surface* properties. One may wonder, for instance, whether altering the surface (and only the surface) may result in a change of $\mathbf{P}$ and/or of $\mathbf{M}$. This very fundamental problem was unsolved until the early 1990s for the electrical case, and until 2005 for the magnetic case.

Condensed matter theory universally adopts *periodic* (a.k.a. Born-von Kármán) boundary conditions (PBCs); in the special case of *crystalline* materials, PBCs lead to the Bloch theorem. One of the virtues of PBCs is that the system has no surface by construction. Therefore whatever one defines or computes within PBCs is by definition "bulk": any surface effect is ruled out. But PBCs *do not* solve our problem, since the (unbounded) position operator $\mathbf{r}$ entering Eq. (13) is a "forbidden" operator, *incompatible* with PBCs. The issue is then how to define and compute $\mathbf{P}$ and $\mathbf{M}$ within PBCs by means of formulas quite different from Eq. (13); therein, in fact, $\rho^{(micro)}(\mathbf{r})$ and $\mathbf{j}^{(micro)}(\mathbf{r})$ are assumed to vanish exponentially outside the finite sample. In the crystalline case, the basic ingredient of such formulas must be the Bloch orbitals of the occupied bands, while the forbidden $\mathbf{r}$ operator must *not* appear.

One important tenet of the modern theory is worth stressing: the macroscopic polarization (magnetization) of a uniformly polarized (magnetized) crystal has *nothing to do* with the lattice-periodical charge (current) distribution—despite contrary statements in several textbooks, Actually, this tenet stems already from classical physics, as emphasized e.g. in the reference work

of Hirst [38].

# 4 DFT, pseudopotentials, and more

The present work reviews the formulations which provide macroscopic electrical polarization and orbital magnetization in condensed matter in terms of single-particle orbitals, which assume the Bloch form in the crystalline case. The formulas are exact for noninteracting electrons, but the obvious aim is to implement them with Kohn-Sham (KS) orbitals, in a given DFT first-principle framework.

Since in this work we need to distinguish between insulators and metals, we stress that we mean "KS insulator" and "KS metal" throughout: that is, we discriminate whether the KS spectrum is gapped or gapless. In the class of "simple" (i.e. computationally friendly) materials a genuine insulator (metal) is also a KS insulator (metal), although pathological cases (computationally unfriendly) do exist.

Having specified this, the key issue is then: Does the KS polarization/magnetization coincide with the physical many-body one? The answer is subtle, and is different whether one chooses either "open" boundary conditions (OBC), as appropriate for molecules and clusters, or PBCs (Born-von Kármán), as appropriate for condensed systems—either crystalline or disordered.

Within OBC the KS orbitals vanish at infinity. For a system of $N$ electrons with $N/2$ doubly occupied orbitals $\varphi_j(\mathbf{r})$ the dipoles (electrical and magnetical) of the fictitious noninteracting KS system are then, in agreement with Eq. (13)

$$\mathbf{d} = \mathbf{d}_{\rm nuclear} - 2e\sum_{j=1}^{N/2}\langle\varphi_j|\mathbf{r}|\varphi_j\rangle, \qquad \mathbf{m} = -\frac{e}{2c}\sum_{j=1}^{N/2}\langle\varphi_j|\mathbf{r}\ \times\mathbf{v}|\varphi_j\rangle, \tag{14}$$

where $\mathbf{v} = i[H,\mathbf{r}]$, and $H$ is the KS Hamiltonian, Atomic Hartree units ($e = \hbar = m_e = 1$) are adopted in most of the following ($c \simeq 137$). The basic tenet of DFT is that the microscopic density of the fictitious noninteracting KS system coincides with the density of the interacting system: hence Eq. (14) provides the exact many-body $\mathbf{d}$ for molecules and clusters. However, when considering a large system in the thermodynamic limit, the density in the surface region contributes *extensively* to the dipole. The magnetic case is different: the microscopic current in the noninteracting KS system *needs not* to be equal to the one in the interacting physical one. The drawback is in principle cured by the Vignale-Rasolt current DFT [39], although a simple, universal, and reliable functional to be applied in actual computations has still to appear [40–42].

The modern theory, as formulated below, provides formulas for $\mathbf{P}$ and $\mathbf{M}$ which are exact within PBCs for noninteracting electrons. However, within PBCs the macroscopic polarization $\mathbf{P}$ is *not* a function of the microscopic density, hence the value of $\mathbf{P}$ obtained from the KS orbitals, in general, is not the correct many-body $\mathbf{P}$. This was first shown in 1995 by Gonze, Ghosez, and Godby [43], and later discussed by several authors. A complete account of the issue can be found in Ref. [10]. Needless to say, the situation for $\mathbf{M}$ is no better.

Therefore, neither $\mathbf{P}$ nor $\mathbf{M}$ can be exactly expressed—even in principle—within standard DFT; but the exact DFT functional is obviously inaccessible, and even sometimes pathological. The

practical issue for the $\Psi_{\mathbf{k}}$ community is whether the current popular flavors of DFT provide an accurate approximation to the experimental values of $\mathbf{P}$ and $\mathbf{M}$ in a large class of materials.

In the electrical case a vast first-principle literature accumulated over the years—by either linear-response theory or the modern theory—typically shows errors of the order of 10-20% on permittivity, and much less on most other properties (infrared spectra, piezoelectricity, ferroelectricity) for many different materials. It is unclear which part of the error is to be attributed to DFT per se, and which part is to be attributed to the *approximations* to DFT. The above mentioned error refers to 3d systems (crystalline, amorphous, and liquid); the state of the art is much worse for quasi 1d systems (polymers) where the polarizabilities and hyperpolarizabilities can be off by orders of magnitude [44]. For such case studies the drawback is shown by computations within OBC, where DFT is in principle exact: hence the culprit is in the *approximate* functional.

In the magnetic case the experience is much more limited, and accumulated only by linear-response theory in the work of Mauri and coworkers [30, 45–48]. For the case studies addressed so far the error seems fairly small.

Next, we switch discussing an issue related to the use of pseudopotentials, where a key difference between the electrical and magnetic case exists. In the former case, the pseudo-wavefunctions contain all of the information (to a very good approximation), and the formalism can be applied as it stands; in fact, it is implemented as such within the pseudopotential codes [13, 14, 16–18]. Quite on the contrary, in the latter case the orbital currents associated to the pseudo-wavefunctions miss very important physical contributions. While all-electron implementations have not yet appeared, the state-of-the art calculations [27, 28] combine the pseudopotential approach with a a Blöchl-like PAW reconstruction for all elements beyond the first row, much in the same way as first shown by Pickard and Mauri in the framework of linear-response theory [46, 48].

## 5 Linear response

As stated in the very first paragraph of this work, we are mostly addressing the modern theory of polarization $\mathbf{P}$ and the modern theory of (orbital) magnetization $\mathbf{M}$. Before the development of the modern theories, *derivatives* of $\mathbf{P}$ and $\mathbf{M}$ where accessible at the first-principle level via linear-response theory. Some (though not all) experimental observables related to $\mathbf{P}$ and $\mathbf{M}$ are by definition derivatives with respect to suitable perturbations. Several observables in this class have been computed over the years for many materials by means of specialized codes (see below).

The spontaneous polarization of a ferroelectric material and, analogously, the spontaneous orbital magnetization of a ferromagnetic material cannot be accessed via linear-response theory. Therefore such observables were ill defined from an electronic-structure viewpoint until the advent of the modern theories. Actually, the first computation ever of the spontaneous polarization of a ferroelectric was published in 1993 [49]. As for orbital magnetization, all computations on the market rely on the uncontrolled muffin-tin approximation; the first implementation of the modern theory (where such approximation is not needed) is appearing nowadays [28].

Even in the cases where the physical observable is by definition a derivative, it proves often convenient to evaluate such derivative as a finite difference by means of the modern theory. This does not require a specialized code, in that it only needs a couple of ground-state calculations. The approach is particularly appealing when studying complex materials and/or using complex forms of exchange-correlation functionals. For instance, infrared spectra of liquids are routinely accessed via the modern theory of polarization [50–52].

### 5.1 Linear-response tensors

We indicate as $F(\mathbf{E},\mathbf{H},\lambda)$ the free energy per unit volume, where $\lambda$ is the short-hand scalar notation for a macroscopic perturbation which is actually tensorial as well (e.g. zone-center phonon, macroscopic strain, &C.). We define $\lambda$ such as $\lambda = 0$ is the equilibrium unperturbed value. We *exclude* from $F$ the free energy of the free fields, which exists even in absence of the material. At any $\lambda$ value the polarization and the magnetization are the derivatives

$$\mathbf{P} = -\frac{dF}{\partial \mathbf{E}}, \qquad \mathbf{M} = -\frac{dF}{\partial \mathbf{H}}, \tag{15}$$

evaluated at $\mathbf{E} = 0$ and $\mathbf{H} = 0$. In this work we tacitly refer to the orbital term only in $\mathbf{M}$.

The linear-response tensors are second derivatives of $F$. In particular $\partial\mathbf{P}/\partial\mathbf{E} = -\partial^2 F/\partial\mathbf{E}\partial\mathbf{E}$ is the electrical susceptibility and $\partial\mathbf{M}/\partial\mathbf{H} = -\partial^2 F/\partial\mathbf{H}\partial\mathbf{H}$ is the magnetic susceptibility. The common symbol $\overleftrightarrow{\chi}$ is customarily used for both tensors. It must be emphasized that the electrical $\overleftrightarrow{\chi}$ is definite positive and of the order one, while the magnetic $\overleftrightarrow{\chi}$ can have either sign and is fairly small, of the order $(1/137)^2$, except near a ferromagnetic transition or in superconducting materials. For this reason $\mathbf{H}$ can be safely replaced with $\mathbf{B}$ in many circumstances.

The evaluation of susceptibilities is performed since several years by means of specialized linear-response codes, and is without reach of the modern theories of polarization and magnetization, at least in their original version. An extension of the theory [31,32], not discussed in this work, removes such limitation in the electrical case. The magnetic case is universally dealt with the long-wavelength linear-response approach of Mauri et al. [30].

The mixed derivative $\overleftrightarrow{\alpha} = -\partial^2 F/\partial\mathbf{E}\partial\mathbf{H} = \partial\mathbf{M}/\partial\mathbf{E} = \partial\mathbf{P}/\partial\mathbf{H}$, named the magnetoelectric polarizability, is much in fashion nowadays given the current high interest in multiferroics (see the April 2009 $\Psi_{\mathbf{k}}$ "Scientific Highlight of the Month" [53]) . It has been discovered very recently (2009) that the orbital magnetoelectric polarizabilty has some very nontrivial topological features [54]. Obviously, no first-principle computation exists.

The remaining linear-response tensors are the mixed second derivatives $\partial\mathbf{P}/\partial\lambda = -\partial^2 F/\partial\lambda\partial\mathbf{E}$ and $\partial\mathbf{M}/\partial\lambda = -\partial^2 F/\partial\lambda\partial\mathbf{H}$ , evaluated at equilibrium ($\lambda = 0$). Specialized linear-response codes [13,16] allow the computation of some of these tensors from first principles; by exploiting the symmetry of the mixed derivatives (Schwarz's theorem) there are usually two different paths, in principle equivalent but computationally very different in their implementation.

The use of a specialized code can be avoided (as said above) by evaluating the $\mathbf{P}$ and $\mathbf{M}$ derivatives as finite differences by means of the modern theories of polarization and magnetization.

### 5.2 Electrical case: pyroelectricity, piezoelectricity, and IR charges

The pyroelectric coefficient is defined as

$$\Pi_\alpha = \frac{dP_\alpha}{dT} \,, \tag{16}$$

the piezoelectric tensor as [55]

$$\gamma_{\alpha\beta\delta} = \frac{\partial P_\alpha}{\partial \epsilon_{\beta\delta}} \,, \tag{17}$$

and the dimensionless Born (or "dynamical" or "infrared") charge as

$$Z^*_{s,\alpha\beta} = \frac{V_\mathrm{c}}{e}\frac{\partial P_\alpha}{\partial u_{s,\beta}} \,, \tag{18}$$

that is as derivatives of $\mathbf{P}$ with respect to temperature $T$, strain $\epsilon_{\beta\delta}$, and displacement $\mathbf{u}_s$ of sublattice $s$, respectively, where $V_\mathrm{c}$ is the primitive cell volume. In the above formulas, derivatives are to be taken at zero electric field and zero strain when these variables are not explicitly involved.

By interpreting the second mixed derivatives of $F$ the other way around, we can define $\Pi$ via the specific heat change linearly induced by a field at constant temperature, $\gamma$ via the macroscopic stress linearly induced by a field at zero strain, and $Z^*$ via the forces linearly induced by a field at the equilibrium geometry. This can be exploited in practice in linear-response calculations.

To the best of author's knowledge, pyroelectricity has never been investigated at the first-principle level in any material, although it is possibly within reach of finite-$T$ Car-Parrinello simulations [56]. The other three tensor properties have been extensively studied in the literature, for many classes of materials, via linear-response theory. The first DFT computation ever of permittivity (for Si) appeared in 1986 [57] and of piezoelectric tensors (for the III-Vs) in 1989 [58]. Nowadays, most state-of-the-art linear-response calculations are based on the so-called "density-functional perturbation theory", as described e.g. in the comprehensive Refs. [59, 60], and implemented in the public-domain codes QUANTUM-ESPRESSO [16] and ABINIT [13].

Linear-response methods, also called—in quantum-chemistry jargon—"analytical derivative" methods, are not the unique tool to compute some of the above derivative properties: numerical differentiation in conjunction with the modern theory can be used as well. Since piezoelectric and infrared tensors are by definition zero-field properties, first-principle studies have widely and successfully used the modern theory within finite-difference schemes, particularly for complex materials, complex basis sets, and nonstandard functionals [61, 62].

Implementations of the modern theory have been been instrumental in the study e.g. of piezoelectric and infrared properties of ferroelectric perovskites [21], as well as of the infrared spectra of liquid and amorphous materials [51, 52].

### 5.3 A closer look at IR charges (Born effective charge tensors)

The Born (or IR) effective charge tensor, Eq. (18), can equivalently be defined (as already observed) as the force $\mathbf{f}_s$ linearly induced on a given nucleus $s$ by a *macroscopic* $\mathbf{E}$ field of unit

magnitude. This force can obviously be expressed as the *microscopic* $\mathbf{E}_s$ field at site $s$, times the bare nuclear charge $eZ_s$:

$$f_{s,\alpha} = eZ^*_{s,\beta\alpha}E_\beta = eZ_sE_{s,\alpha}. \tag{19}$$

Notice that the Cartesian tensor $\overleftrightarrow{Z}^*_s$ is in general nonsymmetric. It follows that the local microscopic field at site $s$ is related to the macroscopic one as

$$\frac{\partial E_{s,\alpha}}{\partial E_\beta} = Z^*_{s,\beta\alpha}/Z_s. \tag{20}$$

In order to proceed further, we adopt in the following of this section an all-electron view (no pseudopotentials): therefore the perturbation induced by the displacement of nucleus $s$ and its periodic replicas by an infinitesimal amount $\mathbf{u}_s$ is identical to introducing in the unperturbed crystal an extra point dipole of magnitude $\mathbf{d}_s = eZ_s\mathbf{u}_s$ (and its periodic replicas), where $Z_s$ is the bare nuclear charge. The original definition of Eq. (18) can thus be recast as

$$Z^*_{s,\alpha\beta}/Z_s = V_{\rm c}\frac{\partial P_\alpha}{\partial d_{s,\beta}}\ . \tag{21}$$

The above manipulations are useful to show that the NMR shielding tensor $\overleftrightarrow{\sigma}_s$, introduced next, is the perfect magnetic analogue of $\overleftrightarrow{Z}^*_s\ /Z_s$.

### 5.4 Magnetic case: NMR shielding tensor

In non magnetic materials, the magnetic susceptibility is of purely orbital nature. Since the pioneering work of Mauri and Louie [30], this property has been successfully computed in many materials via linear response in the long wavelength limit.

Other properties, like the EPR $g$ tensor for paramagnetic defects in solids, are also computed by suitable linear-response techniques which generalize the Mauri et a. approach [63].

NMR spectroscopy [64] has been recognized since 1938 [65] to be a powerful experimental probe of local chemical environments, including structural and functional information on molecules, liquids, and increasingly, on solid-state systems.

The NMR nuclear shielding tensors $\overleftrightarrow{\sigma}_s$ by definition linearly relates the local microscopic magnetic field at a given nucleus $\mathbf{B}_s$ to the external macroscopic field $\mathbf{B}^{(\rm ext)}$ applied to the finite sample:

$$\sigma_{s,\alpha\beta} = \delta_{\alpha\beta} - \frac{\partial B_{s,\alpha}}{\partial B^{(\rm ext)}_\beta}. \tag{22}$$

It obviously depends on the sample shape (see Sec. 2.2); it is expedient to start with a sample in the form of a slab, with $\mathbf{B}^{(\rm ext)}$ normal to the slab, as in the left sketch of Fig. 2. For other shapes a correction is easily computed as a simple function of $\overleftrightarrow{\chi}$. The chosen shape has the virtue that the macroscopic screened field $\mathbf{B}$ inside the sample is equal to the external field $\mathbf{B}^{(\rm ext)}$, hence

$$\sigma_{s,\alpha\beta} = \delta_{\alpha\beta} - \frac{\partial B_{s,\alpha}}{\partial B_\beta}, \tag{23}$$

whose electrical analogue is Eq. (20) with the obvious identification

$$Z^*_{s,\beta\alpha}/Z_s \quad \longleftrightarrow \quad \delta_{\alpha\beta} - \sigma_{s,\alpha\beta}. \tag{24}$$

The linear-response approach of Mauri et al. [45]—called in the following the "direct" approach–exploits Eq. (23) by computing the microscopic orbital currents linearly induced by a long-wavelength **B** field. Many improvements and applications have appeared in the literature since more than a decade from the original paper [46,48]. An alternative approach, based on Wannier functions in a supercell, has also been proposed in 2001 by Sebastiani and Parrinello [66].

Very recently it has been demonstrated how to compute NMR shielding tensor $\overleftrightarrow{\sigma}_s$ via a "converse" approach, by exploiting Schwarz's theorem and the modern theory of magnetization [27]. The logics can be easily explained having in mind the electrical analogue, Sec. 5.3, and Schwarz's theorem. Eqs. (21) and (24) immediately yield

$$\delta_{\alpha\beta} - \sigma_{s,\alpha\beta} = V_{\rm c} \frac{\partial M_\beta}{\partial m_\alpha}, \tag{25}$$

where it is understood that the derivative is taken at zero **B** field. In order to implement Eq. (25) in a first-principle calculation one applies an infinite array of point-like magnetic dipoles $\mathbf{m}_s$ to all equivalent sites and calculates the change in macroscopic orbital magnetization **M** by means of the modern theory. The vector potential corresponding to such perturbation is lattice-periodical (since **B** is zero), and is easily inserted in the crystalline kinetic energy.

The very first test cases studied by this converse approach were some representative molecules in a supercell, crystalline diamond, and liquid water [27]. The induced **M** proves to be linear and stable over nine orders of magnitude, where $\mathbf{m}_s$ varies between $10^{-6}$ to $10^3$ Bohr magnetons. The results compare very favorably with previous results from the direct approach for the same systems [45,67,68].

In the converse approach one needs to perform three calculations for each site, but convergence of the perturbed Hamiltonian (starting from the unperturbed one) is quite fast and one can deal with a cell with hundreds of atoms. The main advantage, however, is that the converse method avoids a linear-response implementation (requiring substantial extra coding) and, furthermore, is implementable with any complex form of exchange-correlation functional, including DFT+U.

# 6 Modern theory of polarization

The modern theory of polarization is at a very mature stage. Several review papers have appeared in the literature. The very first one, Ref. [8], is still an highly cited classic (for crystalline systems); the most recent ones are Refs. [9,10]. Here we summarize the basic concepts and the basic formulas, mostly aiming at comparing them with the modern theory of orbital magnetization, discussed below.

Most textbooks [33,36] provide a flawed definition of **P**, not implementable in practical computations [37]. A change of paradigm emerged in the early 1990s [3,4]; the modern theory, based on a Berry phase, was founded by King-Smith and Vanderbilt soon afterwards [5]. At its foundation, the modern theory was limited to a crystalline system in an independent-electron—either KS or Hartree-Fock—framework. Later, the theory was extended to correlated and/or disordered systems [6,7]. Here we are going to present some of the main formulas in reverse historical order.

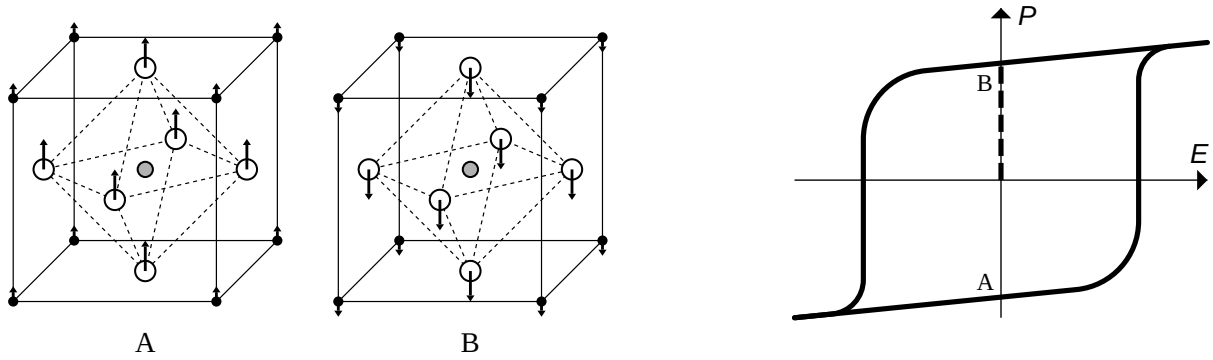


Figure 3: Left: Tetragonal $KNbO_3$. Solid, shaded, and empty circles represent K, Nb, and O atoms, respectively. The internal displacements (magnified by a factor 4) are indicated by arrows for two ($A$ and $B$) enantiomorphous ferroelectric structures. An applied field switches between the two and reverses the polarization. Right: The polarization *difference* is typically measured via an hysteresis loop. The magnitude of the spontaneous polarization is also shown (vertical dashed segment); notice that spontaneous polarization is a zero-field property

The change of paradigm started with realizing that only *differences* of $\mathbf{P}$ are experimentally observable as bulk material properties. This is obvious for the derivative properties listed above; but even the "spontaneous" $\mathbf{P}$ is not accessible as an equilibrium property [3, 4]. In ferroelectric materials one exploits the switchability of $\mathbf{P}$: the quantity actually measured is the *finite difference* $\Delta\mathbf{P}$ between two different structures of the same material. An experimental determination of the spontaneous polarization is normally extracted from a measurement of the transient current flowing through the sample during an hysteresis cycle (Fig. 3).

The modern theory—in agreement with the experiment—avoids addressing the "absolute" polarization of a given equilibrium state, quite in agreement with the experiments, which invariably measure polarization *differences*. Instead, it addresses differences in polarization between two states of the material that can be connected by an adiabatic switching process. The time-dependent Hamiltonian is assumed to remain insulating at all times, and the polarization difference is then equal to the time-integrated transient macroscopic current that flows through the insulating sample during the switching process:

$$\Delta\mathbf{P} = \mathbf{P}(\Delta t) - \mathbf{P}(0) = \int_0^{\Delta t} dt\, \mathbf{j}(t). \tag{26}$$

In the adiabatic limit $\Delta t \to \infty$ and $\mathbf{j}(t) \to 0$, while $\Delta\mathbf{P}$ stays finite. Addressing currents (instead of charges) explains the occurrence of *phases* of the wavefunctions (instead of square moduli) in the modern theory. Eventually the time integration in Eq. (26) will be eliminated, leading to a two-point formula involving only the initial and final states.

### 6.1 Single k-point formula for supercell calculations

For the sake of simplicity we deal with $N$ electrons in a cubic supercell of size $L$. We choose the boundary condition that the microscopic field $\mathbf{E}^{(\mathrm{micro})}(\mathbf{r})$ averages to zero over the supercell (see the discussion in Sec. 2.1), hence the KS potential is supercell-periodic. Notice that such choice corresponds to a vanishing macroscopic field $\mathbf{E}$ only insofar as the sample is homogeneous;

otherwise (e.g. when simulating surfaces, interfaces, and polar molecules) the macroscopic field is in general nonzero in different supercell regions.

Suppose that $\varphi_j(\mathbf{r})$ are the occupied adiabatic eigenstates of the KS instantaneous Hamiltonian at time $t$, normalized to one in the supercell, and obeying PBCs therein; in other words they are obtained from diagonalizing the Hamiltonian at the $\Gamma$ point at time $t$. We define the the $N/2 \times N/2$ connection matrix

$$\mathsf{S}_{\alpha,jj'} = \langle \varphi_j | \mathrm{e}^{i\frac{2\pi r_\alpha}{L}} | \varphi_{j'} \rangle ., \tag{27}$$

which is an implicit function of the adiabatic time; notice that the operator in Eq. (27) is supercell-periodic. The single-point Berry phase is defined as [7, 69, 70]

$$\gamma_\alpha = \mathrm{Im\ ln\ det}\ \mathsf{S}_\alpha; \tag{28}$$

this phase is gauge-invariant, meaning that it is invariant for unitary transformations of the occupied orbitals between themselves.

Suppose that the nuclei are at sites $\mathbf{R}_m$ with charges $Z_m$; when they are adiabatically displaced the transient macroscopic electrical current (nuclear plus electronic) entering Eq. (26) is, in Hartree units,

$$\mathbf{j}(t) = \frac{1}{L^3} \sum_m Z_m \frac{d\mathbf{R}_m}{dt} + \mathbf{j}^{(\mathrm{el})}(t). \tag{29}$$

Notice that the overall charge neutrality of the system ($N = \sum_m Z_m$) is essential for dealing with dipolar properties. It can be shown, by means of linear-response theory, that the $\alpha$-component of the electronic transient current is

$$j_\alpha^{(\mathrm{el})}(t) = -\frac{1}{\pi L^2} \frac{d\gamma_\alpha(t)}{dt}, \tag{30}$$

where $\gamma_\alpha$ is the instantaneous Berry phase of Eq. (28). This equation is correct to leading order in $1/L$ and for double occupancy [7, 69, 70]. Replacing it into Eqs. (26) and (29) we get, in the large-$L$ limit

$$\Delta P_\alpha = \frac{1}{L^3} \sum_m Z_m \Delta R_{m,\alpha} - \frac{1}{\pi L^2} [\gamma_\alpha(\Delta t) - \gamma_\alpha(0)]. \tag{31}$$

This is the two-point formula universally used, e.g. in Car-Parrinello [56] simulations, whenever polarization features are addressed [51, 52]; the generalization to noncubic supercells is trivial.

It is worth noticing that the nuclear and electronic terms contributing to $\Delta\mathbf{P}$ in Eq. (31) are *not* separately invariant for translation of the origin in the supercell. The key point is that their sum is indeed invariant, modulo the "quantum" discussed below, Sec. 6.4.

## 6.2 Many k-point formula for crystalline calculations

Let us assume, for the sake of simplicity, a simple cubic lattice of lattice constant $a$. Then the Born-von-Kàrmàn period $L$ is an integer multiple of the lattice constant: $L = Ma$, where $M \to \infty$ in the large-system limit. The most general crystal structure can be considered by means of a simple coordinate transformation [8]. The KS potential is lattice-periodical, meaning that the macroscopic field $\mathbf{E}$ (i.e. the cell average of the microscopic one) vanishes.

The allowed Bloch vectors are discrete

$$\mathbf{k}_{s_1,s_2,s_3} = \frac{2\pi}{Ma}(s_1, s_2, s_3), \qquad s_\alpha = 0, 1, \dots M-1,$$

and the corresponding Bloch orbitals are $\psi_{n\mathbf{k}_{s_1,s_2,s_3}}(\mathbf{r}) = \mathrm{e}^{i\mathbf{k}_{s_1,s_2,s_3}\cdot\mathbf{r}} u_{n\mathbf{k}_{s_1,s_2,s_3}}(\mathbf{r})$. The overlap matrix of Eq. (27) becomes then

$$\begin{aligned} \mathsf{S}_{\alpha,jj'} &\rightarrow \frac{1}{M^3}\int_0^L dx \int_0^L dy \int_0^L dz\ \psi^*_{n\mathbf{k}}(\mathbf{r})\mathrm{e}^{i\frac{2\pi r_\alpha}{Ma}}\psi_{n'\mathbf{k}'}(\mathbf{r}) \\ &= \int_0^a dx \int_0^a dy \int_0^a dz\ u^*_{n\mathbf{k}}(\mathbf{r})\mathrm{e}^{i(\mathbf{k}'-\mathbf{k}+\frac{2\pi r_\alpha}{Ma})}u_{n'\mathbf{k}'}(\mathbf{r}), \end{aligned} \tag{32}$$

where $\mathbf{k}$ and $\mathbf{k}'$ must be chosen within the discrete set. The $1/M^3$ factor owes to the fact that the $\varphi_j(\mathbf{r})$ orbitals entering Eq. (27) are normalized in the cube of volume $L^3$, while the Bloch orbitals $\psi_n$ and $u_n$ are normalized in the crystal cell of volume $a^3$. For given $\mathbf{k}$ and $\mathbf{k}'$ the size of the matrix on the rhs of Eq. (32) is $n_\mathrm{b}$ (the number of double-occupied bands), while the $\mathbf{k}$ and $\mathbf{k}'$ arguments run over $M^3$ discrete values. In fact, the total number of electrons in the Born-von-Kàrmàn box is $N = 2n_\mathrm{b}M^3$.

The key difference between the noncrystalline case and the crystalline one is that the connection matrix, Eq. (32), becomes very sparse in the latter case. Focussing, without loss of generality, on the $x$-component ($\alpha = 1$), and writing explicitly $\mathbf{k} = \mathbf{k}_{s_1,s_2,s_3}$ and $\mathbf{k}' = \mathbf{k}_{s'_1,s'_2,s'_3}$, its only nonzero elements are those with $s_1 = s'_1 + 1$, $s_2 = s'_2$, and $s_3 = s'_3$. With the usual definition of the scalar product between $u_n$ orbitals

$$\langle u_{n\mathbf{k}}|u_{n'\mathbf{k}'}\rangle = \int_\mathrm{cell} d\mathbf{r}\ u^*_{n\mathbf{k}}(\mathbf{r})u_{n'\mathbf{k}'}(\mathbf{r}),$$

these nonzero elements can be rewritten as

$$S_{nn'}(\mathbf{k}_{s_1+1,s_2,s_3}, \mathbf{k}_{s_1,s_2,s_3}) = \langle u_{n\mathbf{k}_{s_1+1,s_2,s_3}}|u_{n'\mathbf{k}_{s_1,s_2,s_3}}\rangle\ .$$

Owing to such sparseness, the determinant of the large matrix $\mathsf{S}_x$ (of size $N/2 = n_\mathrm{b}M^3$) in Eq. (27) factorizes into the product of $M^3$ determinants of the small matrices $S(\mathbf{k}, \mathbf{k}')$ (of size $n_\mathrm{b}$ each). The Berry phase defined in Eq. (28) becomes then

$$\begin{aligned} \gamma_x &= \mathrm{Im\ ln} \prod_{s_1,s_2,s_3=0}^{M-1} \det\ S(\mathbf{k}_{s_1+1,s_2,s_3}, \mathbf{k}_{s_1,s_2,s_3}) \\ &= -\sum_{s_2,s_3=0}^{M-1} \mathrm{Im\ ln} \prod_{s_1=0}^{M-1} \det\ S(\mathbf{k}_{s_1,s_2,s_3}, \mathbf{k}_{s_1+1,s_2,s_3}). \end{aligned} \tag{33}$$

If we use the symbol $\boldsymbol{\tau}_\ell$ for the nuclear positions in the unit cell, the main polarization formula, Eq. (31), becomes

$$\Delta P_x = \frac{1}{a^3}\sum_\ell Z_\ell \Delta\tau_{\ell,x} - \frac{1}{\pi M^2 a^2}[\gamma_x(\Delta t) - \gamma_x(0)], \tag{34}$$

and analogously for the other Cartesian components. This is the key formula implemented in most electronic-struture codes for crystalline calculations [13, 15, 16, 18]..

We notice that the $u_{nk}$ orbitals entering $\mathsf{S}$, Eq. (32), can be chosen with arbitrary phase factors (choice of the "gauge"), but these factors cancel out in Eq. (33), leaving no arbitrariness. Even more, Eq. (33) is invariant by unitary transformations of the occupied orbitals at a given $\mathbf{k}$. Therefore the discrete Berry phase in Eq. (33) is a global property of the occupied manifold as a whole; this is useful when the band numbering is nonunique (e.g in the case of band crossings).

### 6.3 King-Smith & Vanderbilt formula

In order to make contact with the original continuum formulation by King-Smith and Vanderbilt it is expedient to define $\gamma_\alpha^{(\mathrm{crys})} = \gamma_\alpha / M^2$, and rewite Eq. (34) as

$$\Delta P_x = \frac{1}{a^3} \sum_\ell Z_\ell \Delta\tau_{\ell,x} - \frac{1}{\pi a^2} [\gamma_x^{(\mathrm{crys})}(\Delta t) - \gamma_x^{(\mathrm{crys})}(0)], \tag{35}$$

In the $M \to \infty$ limit the $\mathbf{k}$-point mesh becomes dense. If the gauge is chosen in such a way that the overlap matrix $S_{nn'}(\mathbf{k}, \mathbf{k}') = \langle u_{n\mathbf{k}} | u_{n'\mathbf{k}'} \rangle$ is a differentiable function of its arguments, the electronic term in Eq. (35) converges to a reciprocal-cell integral. In fact it can be shown that, in the $M \to \infty$ limit [5, 8, 70]

$$\gamma_x^{(\mathrm{crys})} = -\lim \frac{1}{M^2} \sum_{s_2,s_3=0}^{M-1} \mathrm{Im}\ \ln \prod_{s_1=0}^{M-1} \det\, S(\mathbf{k}_{s_1,s_2,s_3}, \mathbf{k}_{s_1+1,s_2,s_3}) \tag{36}$$

$$\to \frac{ia^2}{(2\pi)^2} \int d\mathbf{k}\, \frac{\partial}{\partial k'_x} \sum_{n=1}^{n_\mathrm{b}} S_{nn}(\mathbf{k}, \mathbf{k}') \Big|_{\mathbf{k}'=\mathbf{k}} = \frac{ia^2}{(2\pi)^2} \int d\mathbf{k} \sum_{n=1}^{n_\mathrm{b}} \langle u_{n\mathbf{k}} | \frac{\partial}{\partial k_x} u_{n\mathbf{k}} \rangle. \tag{37}$$

Historically, Eqs. (36) and (37) were derived first by King-Smith and Vanderbilt [5], and the single-point formula, Eq. (31), much later [7].

For the sake of completeness, we give also the formula for the most general crystalline lattice, with double band occupation. The electronic contribution to electronic polarization is the Brillouin-zone (BZ) integral

$$\mathbf{P}^{(\mathrm{el})} = -\frac{2i}{(2\pi)^3} \int_{\mathrm{BZ}} d\mathbf{k} \sum_{n=1}^{n_\mathrm{b}} \langle u_{n\mathbf{k}} | \nabla_{\mathbf{k}} u_{n\mathbf{k}} \rangle, \tag{38}$$

where it is understood that the expression must be used to evaluate polarization *differences* in a two-point formula, and the sum is over the occupied bands. The formula given here is in atomic Hartree units, for double occupancy, and for orbitals normalized to one over the crystal cell. The integral is over the BZ or, equivalently, over a reciprocal cell.

We remind that polarization (as a bulk material property) only makes sense in insulators, and that, in this work, we refer more precisely to "KS insulators". In fact, the integration is Eqs. (37) and (38) is over the whole reciprocal cell or, equivalently, over the whole BZ. The spectrum has a gap and the number $n_\mathrm{b}$ of occupied orbitals is independent of $\mathbf{k}$. Also, it is worth noticing that the integrand in Eqs. (37) and (38) is *not* gauge-invariant, in that it depends on the (arbitrary) choice of the phases of $|u_{n\mathbf{k}}\rangle$ at different $\mathbf{k}$'s; nonetheless the integral *is* gauge-invariant (modulo the "quantum" discussed below). More generally, the integral is invariant for any differentiable unitary mixing of the occupied $|u_{n\mathbf{k}}\rangle$ between themselves at a given $\mathbf{k}$. A similar observation was made above about the discrete Eq. (33).

### 6.4 The polarization "quantum"

Given that every phase is defined modulo $2\pi$, all of the two-point formulas for $\Delta\mathbf{P}$ in terms of Berry phases are arbitrary modulo a polarization "quantum". This is the tradeoff one has to pay when switching from the adiabatic-connection formula, Eq. (26)—where no such arbitrariness exists—to any of the two-point formulas given above.

In the single **k**-point case, Eq. (31), the 'quantum" is $2/L^2$: since we are interested in the large supercell limit, where the "quantum" vanishes, the two-point formula is apparently useless. This is not the case, and in fact Eq. (31) is routinely used for evaluating polarization differences in noncrystalline materials. The key point is that the $L \to \infty$ limit is not actually needed; for an accurate description of a given material, it is enough to assume a *finite* $L$, actually larger than the relevant correlation lengths in the material. For any given length, the polarization "quantum" $2/L^2$ sets an upper limit to the magnitude of a polarization difference accessible via the two-point formula, Eq. (31). The larger are the correlation lengths, the smaller is the accessible $\Delta\mathbf{P}$. This is no problem at all in practice, either when evaluating static derivatives by numerical differentiation, such as e.g. in Ref. [50, 71], or when performing Car-Parrinello simulations [51,52]. In the latter case $\Delta t$ is a Car-Parrinello time step (a few a.u.), during which the polarization varies by a tiny amount, much smaller than the quantum $2/L^2$ (the tipical size of a large simulation cell nowadays is $L \simeq 50$ a.u.). Whenever needed, the drawback may be overcome by splitting $\Delta t$ in Eq. (26) into several smaller time intervals, and by using the two-point formula for each of them.

It is worth emphasizing that—owing to supercell periodicity—even the classical nuclear term in Eq. (31) is affected by a similar indeterminacy, whenever a nuclear displacement $\Delta\mathbf{R}_m$ becomes of order $L$.

In the crystalline case translational invariance produces the much larger "quantum" $2/a^2$. In fact, it is easily shown that Eq. (37) is gauge-invariant modulo $2\pi$. The classical nuclear term has a similar indeterminacy.

Caution is in order in numerical work, when using Eq. (36) at finite $M$, since in general the $|u_{n\mathbf{k}}\rangle$ obtained from numerical diagonalization at the mesh points are *not* differentiable functions of **k**. If each of the $M^2$ terms in the sum is chosen with arbitrary modulo $2\pi$ freedom, then $\gamma_\alpha^{(\mathrm{crys})}$ is unavoidably arbitrary modulo $2\pi/M^2$. A more clever choice is possible (and actually performed in practical implementations) as follows. One starts choosing arbitrarily one of the possible (modulo $2\pi$) values for the first term in the sum ($s_2 = 0$ and $s_3 = 0$); for the remaining terms, it is possible to impose that nearest-neighbor phases differ by much less than $2\pi$ (if the mesh is dense enough). This choice is unique, and eliminates any residual arbitrariness, corresponding to the discrete average of a *continuous* function of $k_y k_z$, as indeed in Eq. (37). By this token the discrete Berry-phase formula, Eq. (36), leads to the polarization "quantum" $2/a^2$ (independent of $M$ and $L$), indeed identical to the continuous one, and large enough to be harmless for most computations.

### 6.5 Wannier functions

The KS ground state is a Slater determinant of doubly occupied orbitals; any unitary transformation of the occupied states among themselves leaves the determinantal wavefunction invariant (apart for an irrelevant phase factor), and hence it leaves invariant any KS ground-state property.

For an insulating crystal, the KS orbitals are the Bloch states of completely occupied bands; these can be tranformed to localized Wannier orbitals (or functions) WFs. This is known since 1937 [72], but for many years the WFs have been mostly used as a formal tool; they became

a popular topic in computational electronic structure and within the $\Psi_{\mathbf{k}}$ community only after the seminal work of Marzari and Vanderbilt [73]; a comprehensive review appeared as the June 2003 $\Psi_{\mathbf{k}}$ "Scientific Highlight of the Month" [74]. If the crystal is metallic, the WFs can still be technically useful, but it must be emphasized that the ground state *cannot* be written as a Slater determinant of localized orbitals of any kind, as a matter of principle [75].

The transformation of the Berry phase formula Eq. (38) in terms of WFs provides an alternative, and perhaps more intuitive, viewpoint. The formal transformation was known since the 1950s [76], although the physical meaning of the formalism was not understood until the seminal work of King-Smith and Vanderbilt.

The unitary transformation which defines the WF $w_{n\mathbf{R}}(\mathbf{r})$, labeled by band $n$ and unit cell $\mathbf{R}$, within our normalization is

$$|w_{n\mathbf{R}}\rangle = \frac{V_{\rm c}}{(2\pi)^3}\int_{\rm BZ} d\mathbf{k}\ {\rm e}^{i\mathbf{k}\cdot\mathbf{R}}\ |\psi_{n\mathbf{k}}\rangle\ . \tag{39}$$

If one then defines the" Wannier centers" as $\mathbf{r}_{n\mathbf{R}} = \langle w_{n\mathbf{R}}|\mathbf{r}|w_{n\mathbf{R}}\rangle$, it is rather straightforward to prove that Eq. (38) is equivalent to

$$\mathbf{P}^{\rm (el)} = -\frac{2}{V_{\rm c}}\sum_{n=1}^{n_{\rm b}} \mathbf{r}_{n\mathbf{0}}. \tag{40}$$

This means that the electronic term in the macroscopic polarization $\mathbf{P}$ is (twice) the dipole of the Wannier charge distributions in the central cell, divided by the cell volume. The nuclear term is obviously similar in form to Eq. (40).

WFs are severely gauge-dependent, since the phases of the $|\psi_{n\mathbf{k}}\rangle$ appearing in Eq. (39) can be chosen arbitrarily. However, their centers are gauge-invariant modulo $\mathbf{R}$ (a lattice vector). Therefore $\mathbf{P}^{\rm (el)}$ in Eq. (40) is affected by the same "quantum" indeterminacy discussed above.

# 7 Geometrical issues

## 7.1 Chern invariants and topological insulators

It has been observed that macroscopic polarization (as a bulk material property) only makes sense in insulating materials, while macroscopic orbital magnetization exists both in insulators and metals. Furthermore, magnetic insulators come in two classes: the "nonexotic" and the "exotic" ones, called in the following "normal insulators" and "topological insulators", respectively.

Until recently the only known realization of a topological insulator was the quantum Hall effect (QHE): a 2d electron fluid in a perpendicular $\mathbf{B}$ field exibits a new state of matter. The "bulk" of the system is insulating, but there are circulating edge states which are robust ("topologically protected") in presence of disorder, and are responsible for the famous plateaus in the transverse conductivity. The same electron fluid can be described using toroidal boundary conditions, where no edge exists. In this case the signature of the quantum Hall state is a topological integer $C_1$ (Chern number of the first class) which geometrically characterizes the wavefunction. The Chern

number is defined below, Eq. (42), and $C_1 = 0$ means a normal insulator. The Hall conductivity in the QHE regime is simply expressed in atomic Hartree units as

$$\sigma_{\rm T} = -C_1/2\pi, \tag{41}$$

or, in ordinary units, $\sigma_{\rm T} = -C_1 e^2/h$.

This result is due to Thouless and coworkers, both in the case of integer [77] and fractional [78] QHE. These two milestone papers mark the debut of geometrical concepts in electronic structure theory [79]. Notice that in the QHE regime, due to the presence of a macroscopic **B** field, the Hamiltonian *cannot* be lattice periodical.

A subsequent breakthrough on the theory side is the Haldane model Hamiltonian [80]: it is comprised of a 2d honeycomb lattice with two tight-binding sites per primitive cell with site energies $\pm\Delta$, real first-neighbor hoppings $t_1$, and complex second-neighbor hoppings $t_2 e^{\pm i\varphi}$, as shown in Fig. 4. Within this two-band model, one deals with insulators by taking the lowest band as occupied. The appeal of the model is that there is no macroscopic field, hence the vector potential and the Hamiltonian are lattice periodical and the single-particle orbitals always have the usual Bloch form. Essentially, the microscopic magnetic field can be thought as staggered (i.e. up and down in different regions of the cell), but its cell average vanishes. As a function of the flux parameter $\phi$, this system undergoes a transition from zero Chern number (i.e. normal insulator) to $|C_1| = 1$ (i.e. topological insulator).

In general, the Chern number for *any* lattice-periodical Hamiltonian in 2d is expressed in terms of the Bloch orbitals as

$$C_1 = \frac{i}{2\pi} \sum_{n=1}^{n_{\rm b}} \int_{\rm BZ} d\mathbf{k} \, [\, \langle \partial u_{n\mathbf{k}}/\partial k_1 \,|\, \partial u_{n\mathbf{k}}/\partial k_2 \rangle - \langle \partial u_{n\mathbf{k}}/\partial k_2 \,|\, \partial u_{n\mathbf{k}}/\partial k_1 \rangle \,], \tag{42}$$

where the sum is over the occupied $n$'s only, and the integral is over the 2d Brillouin zone (the formula here is given for single band occupancy). It is easily verified that $C_1$ is dimensionless, and in fact is quantized in integer units.

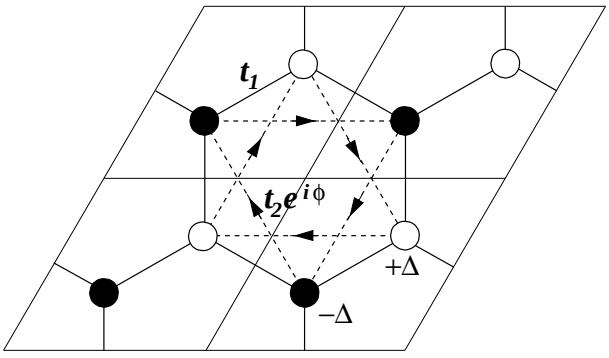


Figure 4: Four unit cells of the Haldane model [80]. Filled (open) circles denote sites with $E_0 = -\Delta$ ($+\Delta$). Solid lines connecting nearest neighbors indicate a real hopping amplitude $t_1$; dashed arrows pointing to a second-neighbor site indicates a complex hopping amplitude $t_2 e^{i\phi}$. Arrows indicate sign of the phase $\phi$ for second-neighbor hopping.

In 3d the Chern number, Eq. (42), is generalized to the (vector) Chern invariant

$$\mathbf{C} = \frac{i}{2\pi} \sum_{n=1}^{n_\mathrm{b}} \int_{\mathrm{BZ}} d\mathbf{k}\, \langle \partial_{\mathbf{k}} u_{n\mathbf{k}}| \times |\partial_{\mathbf{k}} u_{n\mathbf{k}}\rangle, \tag{43}$$

with the usual meaning of the cross product between three-component bra and ket states. Here the integral is over the 3d Brillouin zone, and $\partial_{\mathbf{k}} = \partial/\partial\mathbf{k}$. The Chern invariant has the dimension of an inverse length, and in fact is quantized in units of reciprocal lattice vectors. Notice the analogy with—but also the key difference from—the Berry-phase formula in the modern theory of polarization, Eq. (38).

Whenever the Chern invariant (number in 2d) is nonzero in a periodic Hamiltonian the bulk states are gapped, but there are topologically protected surface (edge in 2d) states which are conducting: we call "Chern insulator" this kind of topological insulator. It is worth noticing that in a Chern insulator Wannier functions *cannot* exist [81] (despite the fact that the Hamiltonian eigenstates do have the Bloch form).

Until recently no experimental realization of an insulator with nonzero Chern number (in 2d) or nonzero Chern invariant (in 3d), *in absence of a macroscopic* $\mathbf{B}$ *field* was known. All known real materials were either conductors or normal insulators, and the exotic insulators remained a curiosity of academic interest only. A mesoscopic 2d Chern insulator, in the same spirit as the Haldane model Hamiltonian, was synthesized in 2008 [82].

The interest in topological insulators has boomed in the last couple of years, and a genuine revolution is underway in two directions: (i) other, more complex topological invariants have been proposed [83, 84]; and (ii) the experimental realization of a topological insulator in 2d and 3d has been demonstrated. This exciting new field is clearly beyond the scope of the present review. We quote only a few very recent references for orientation [85–87].

### 7.2 Berry curvature and the anomalous Hall effect

The integrand in Eqs. (42) and (43) is a key geometrical feature of the wavefunction within PBCs, and goes under the name of "Berry curvature" (in both 2d and 3d), or, equivalently, of "gauge field". We define it per band, i.e.

$$\mathbf{\Omega}_n(\mathbf{k}) = i\langle \partial_{\mathbf{k}} u_{n\mathbf{k}}| \times |\partial_{\mathbf{k}} u_{n\mathbf{k}}\rangle = -\mathrm{Im}\, \langle \partial_{\mathbf{k}} u_{n\mathbf{k}}| \times |\partial_{\mathbf{k}} u_{n\mathbf{k}}\rangle; \tag{44}$$

equivalently one can define the Berry curvature as the antisymmetric Cartesian tensor

$$\Omega_{n,\alpha\beta}(\mathbf{k}) = -2\,\mathrm{Im}\, \langle \partial u_{n\mathbf{k}}/\partial k_\alpha \,|\, \partial u_{n\mathbf{k}}/\partial k_\beta\rangle. \tag{45}$$

The Berry curvature is gauge invariant, hence in principle it leads to observable effects.

In presence of time-reversal symmetry the Chern invariant vanishes, i.e. the Berry curvature integrates to zero over the BZ. However, it is identically zero only in centrosymmetric crystals. Instead, in crystals which are time-reversal symmetric but non centrosymmetric, $\mathbf{\Omega}_n(\mathbf{k})$ contributes to the semiclassical equation of transport [88].

When time-reversal symmetry is broken and the system is metallic the integral of $\mathbf{\Omega}_n(\mathbf{k})$ over the occupied states provides a sizeable contribution to the anomalous Hall effect (AHE), discussed in the following.

In absence of time-reversal symmetry (e.g. in a metallic ferromagnet) the transverse conductance is nonzero even in zero magnetic field. This is the AHE, discovered by E. R. Hall in 1881 (at about the same time as the normal Hall effect); it gathered a renewal of interest in the 2000s. The effect is due to several mechanisms, some of them extrinsic, and the relative role of the different mechanisms is still controversial; however, one important term in the AHE conductivity is intrinsic and purely geometrical. Using Eq. (45) this term is (in atomic Hartree units and for single band occupancy)

$$\sigma_{\alpha\beta} = -\frac{1}{(2\pi)^3} \sum_n \int_{\mathrm{BZ}} d\mathbf{k} \;\; f_{n\mathbf{k}} \Omega_{n,\alpha\beta}(\mathbf{k}), \tag{46}$$

where $f_{n\mathbf{k}} = \theta(\mu - \epsilon_{n\mathbf{k}})$ is the Fermi occupancy factor at $T = 0$, and $\mu$ is the Fermi energy. A formula similar, though not identical, to Eq. (46), was proposed as early as 1954 by Karplus and Luttinger [89]. The genuine Berry-connection formula, Eq. (46), was established in 2002 [90], and implemented in first-principle calculations soon afterwards [91–93] for the three ferromagnetic metals Fe, Co, and Ni.

It is worth pointing out that the 2d analogue of Eq. (46), when applied to a gapped crystal, coincides exactly with the QHE formula, Eq. (41). In both the QHE and AHE cases these topological formulas, derived within PBCs for a sample without boundaries, correspond to dissipationless boundary currents in finite samples.

# 8 Modern theory of magnetization

First of all we remind that both spin and orbital motion of the electrons contribute to the total magnetization. While spin magnetization can be calculated with high accuracy by standard state-of-the-art method as the spin-density functional theory (SDFT), orbital magnetization is the subject of investigations in progress at the fundamental level. In this work, we refer to $\mathbf{M}$ as to the macroscopic orbital magnetization in zero $\mathbf{B}$ field. This requires breaking of time-reversal symmetry in the spatial wavefunction, which can occur in several ways. An important paradigm is the 2d model Hamiltonian introduced by Haldane in 1988 [80] (Fig. 4); in real materials the time-reversal symmetry breaking can be due to spin-orbit interactions (as in ferromagnets), or to an explicit perturbation in nonmagnetic materials (as e.g. detailed in Sec. 5.4).

## 8.1 Normal insulators

In a normal insulator (i.e. whenever the Chern invariant is zero) the Bloch orbitals can be chosen so as to obey $|\psi_{n\mathbf{k}+\mathbf{G}}\rangle = |\psi_{n\mathbf{k}}\rangle$ (the so-called periodic gauge), which in turn warrants the existence of WFs enjoying the usual properties. Under this condition, the formula yielding the macroscopic orbital magnetization in vanishing macroscopic $\mathbf{B}$ field is

$$\mathbf{M} = \frac{1}{c(2\pi)^3} \,\mathrm{Im} \sum_{n=1}^{n_\mathrm{b}} \int_{\mathrm{BZ}} d\mathbf{k} \; \langle \partial_{\mathbf{k}} u_{n\mathbf{k}}| \times \left( H_{\mathbf{k}} + \epsilon_{n\mathbf{k}} \right) |\partial_{\mathbf{k}} u_{n\mathbf{k}}\rangle \; . \tag{47}$$

The formula as given here is in atomic Hartree units ($c \simeq 137$) and for double band occupancy. As usual, $|u_{n\mathbf{k}}\rangle$ is the periodic part in a Bloch orbital, $\epsilon_{n\mathbf{k}}$ is the band energy, and $H_{\mathbf{k}}$ is the effective Hamiltonian acting on the $u$'s, i.e. $H_{\mathbf{k}} = \mathrm{e}^{-i\mathbf{k}\cdot\mathbf{r}} H \mathrm{e}^{i\mathbf{k}\cdot\mathbf{r}}$. The orbitals are normalized to

one over the crystal cell of volume $V_c$; the sum is over the occupied bands and the integral is over the whole BZ.

Eq. (47) has been first established for the single band case, independently in Ref. [11] (via the semiclassical method) and in Ref. [12] (addressing the ground state in term of WFs). In the latter case, computer simulations based on the 2d Haldane model Hamiltonian (Fig. 4) have been instrumental in order to arrive at the magnetization formula and to validate it. A precursor work, appeared in 2003 [94], provides the correct formula for the special case of the Hofstadter model Hamiltonian. The (nontrivial) extension to the many-band case, as given in Eq. (47), was provided in 2006 by Ceresoli et al. [22] (again, via WFs).

It is expedient to compare Eq. (47) with its electrical analogue, which is the King-Smith and Vanderbilt polarization formula, written in Eq. (38) (for double band occupancy and in atomic units as well). The main ingredient in both formulas are **k**-derivatives of the periodic $|u_{n\mathbf{k}}\rangle$ orbitals; additionally, the Hamiltonian and the band energies appear in **M**. A key difference is that in Eq. (38) the *integrand* is gauge-dependent, and only the *integral* is gauge-invariant; in the magnetic case, instead, both the integrand and the integral are gauge-invariant. In the electrical case only the BZ integral—as in Eq. (38)—makes sense, and this is in agreement with the fact that bulk polarization **P** is well defined only in insulators (within our KS scheme, in "KS insulators", to be more precise). In the magnetic case, instead, the same integral appearing in Eq. (47), but limited to states below the Fermi level in metals, is gauge invariant and could make physical sense, since **M** is well defined even in metals. The actual formula for metals (see below, Sec. 8.3) is similar, but somewhat different. A further key difference, worth emphasizing, is that there is no "quantum" indeterminacy in the magnetic case.

An apparent paradox is that Eq. (47) does not appear at first sight to be invariant with respect to translation of the energy zero. However, the zero-Chern-invariant condition—compare Eq. (47) to Eq. (43)—enforces such invariance in any normal insulator.

The main magnetization formula, Eq. (47), for the orbital magnetization of a crystalline insulator can easily be implemented in existing first-principle electronic structure codes, making available the computation of the orbital magnetization in crystals and at surfaces. The **k**-derivatives therein must be discretized as finite differences; a gauge-invariant numerical algorithm to this aim is detailed in Appendix A of Ref. [22].

## 8.2 Single k-point formula for supercell calculations

We start observing that Eq. (47) is invariant by cell doubling. In fact, starting with a cell (or supercell) of given size, we may regard the same physical system as having double periodicity (in all directions), in which case the integration domain in Eq. (47) gets "folded" and shrinks by a factor 1/8, while the number of occupied eigenstates gets multiplied by a factor of 8. It is easy to realize that these are in fact *the same* eigenstates as in the unfolded case, apart possibly for a unitary transformation, irrelevant here. As for the discretized form of Eq. (47), it can be chosen to be numerically invariant by cell doubling within the computational tolerance chosen (by a suitable choice of the mesh).

The supercell is the obvious way of dealing with disordered systems, which can be regarded as

a crystalline systems of large enough size. The actually required size depends on the relevant correlation lengths in the material addressed.

If we replace $V_c$ in Eq. (47) with a (large) supercell volume $V$, the integral is approximated by the value of the integrand at $\mathbf{k} = 0$ times the reciprocal volume $(2\pi)^3/V$. If there are $N$ electrons in the supercell the formula is

$$\mathbf{M} = \frac{1}{cV} \,\mathrm{Im} \sum_{n=1}^{N/2} \langle \partial_{\mathbf{k}} u_{n0}| \times (\, H_0 \, + \epsilon_{n0} \,) \, |\partial_{\mathbf{k}} u_{n0}\rangle \ . \tag{48}$$

This formula has been proposed in Ref. [26] and validated, once more, via simulations based on the 2d Haldane model Hamiltonian. One key virtue of Eq. (48) is its gauge invariance in a generalized sense, that is for arbitrary unitary mixing of the occupied $|u_{n\mathbf{k}}\rangle$ among themselves.

The $\mathbf{k} = 0$ derivatives $|\partial_{\mathbf{k}} u_{n0}\rangle$ appearing in Eq. (48) deserve further discussion, since here we no longer have any mesh, only *one* reciprocal point (the $\Gamma$ point). One possible approach is to evaluate such derivatives via perturbation theory, i.e.

$$|\partial_{\mathbf{k}} u_{n0}\rangle = \sum_{m \neq n} |u_{m0}\rangle \frac{\langle u_{m0}|\mathbf{v}|u_{n0}\rangle}{\epsilon_{m0} - \epsilon_{n0}} \ , \tag{49}$$

where $\mathbf{v}$ is the velocity operator

$$\mathbf{v} = i[H, \mathbf{r}] = \nabla_{\mathbf{k}} H_{\mathbf{k}}|_{\mathbf{k}=0} \ . \tag{50}$$

Eq. (49) is convenient for tight-binding implementations, where the sum is over a small number of terms. We also notice that the matrix representation of $\mathbf{r}$, for use in Eq. (50), is usually taken to be diagonal on the tight-binding basis.

However, Eq. (49) is not convenient for a first-principle implementation, since it would require the evaluation of slowly convergent perturbation sums. This can be avoided taking a different approach. If If $\mathbf{b}_j$ are the shortest reciprocal vectors of the supercell, and $\partial_j$ indicates the partial $\mathbf{k}$-derivative in the direction of $\mathbf{b}_j$, then by definition

$$|\partial_j u_{n0}\rangle = \lim_{\lambda \to 0} \frac{1}{\lambda |\mathbf{b}_j|} ( \, |u_{n\,\lambda \mathbf{b}_j}\rangle - |u_{n0}\rangle \, ). \tag{51}$$

For a large enough supercell, the limit is approximated by taking $\lambda = 1$. Next we wish to evaluate $|u_{n\mathbf{b}_j}\rangle$ without actually diagonalizing the Hamiltonian at $\mathbf{k} \neq 0$. To this aim, we notice that the state $\mathrm{e}^{-i\mathbf{b}_j \cdot \mathbf{r}} |u_{n0}\rangle$ obeys periodic boundary conditions and is an eigenstate of $H_{n\mathbf{b}_j}$ corresponding, possibly, to a different occupied eigenvalue and to a different phase choice. In other words, no further diagonalization is needed to identify the manifold spanned by the occupied eigenstates $|u_{n\mathbf{b}_j}\rangle$ appearing in Eq. (51). It is then easy to evaluate Eq. (48), provided a specific gauge is enforced. In fact, Eq. (48) is gauge invariant by unitary mixing of the occupied eigenstates. We further observe that the eigenstates $|u_{n\mathbf{k}}\rangle$ obtained from numerical diagonalization are *not* analytical functions of $\mathbf{k}$—as instead is implicitly assumed in Eq. (51). But this feature makes no harm after the gauge transformation is performed. The algorithm performing the required gauge transformation is detailed in Ref. [26], and is ispired by Refs. [95, 96].

The single-point formula, Eq. (48), has been implemented in a first-principle framework to evaluate the NMR shielding tensor in liquid water, via the converse approach discussed in Sec. 5.4 [27].

The formula is ideally suited for implementation in time-dependent Car-Parrinello simulations, as in the corresponding electrical case (Sec. 6.1), but an important caveat is in order. Whenever time-reversal symmetry is absent, the *classical* nuclear equation of motion needs to be modified by the occurrence of a vector potential of geometric origin (or "gauge potential") entering the nuclear kinetic energy. For more details, see Sec. 5.2 in Ref. [70].

### 8.3 Chern insulators and metals

We switch here to single band occupancy, having in mind e.g. a ferromagnet (where the orbitals for up and down spins are different). The macroscopic magnetization per spin channel is

$$\mathbf{M} = \frac{1}{2c(2\pi)^3}\ \mathrm{Im} \sum_n \int_{\mathrm{BZ}} d\mathbf{k}\ f_{n\mathbf{k}} \langle \partial_{\mathbf{k}} u_{n\mathbf{k}}| \times (\ H_{\mathbf{k}} + \epsilon_{n\mathbf{k}} - 2\mu\ ) |\partial_{\mathbf{k}} u_{n\mathbf{k}}\rangle\ , \tag{52}$$

where $f_{n\mathbf{k}}$ is, as above, the Fermi occupancy factor at $T = 0$ and $\mu$ is the Fermi energy. The formula applies to both Chern insulators (defined as insulators with nonzero Chern invariant) and metals. Eq. (52) is obviously invariant by translation of the energy zero and coincides with (one half of) Eq. (47) in the case of a normal insulator. In fact, the role of $\mu$ is irrelevant if the Chern invariant, Eq. (43), vanishes. In both Chern insulators and metals the magnetization depends on $\mu$, as it must be (see Sec. 8.4).

Eq. (52) was first derived from semiclassical arguments for the single-band case in Ref. [11]. Subsequently, Eq. (52) was heuristically assumed in Ref. [22] and validated via computer experiments. Needless to say, the transformation to WFs leading to the proof of Eq. (47) could not be used for Chern insulators and for metals.

The numerical validation of Eq. (52) was based once more on the 2d Haldane model Hamiltonian (Fig. 4) at various fillings, and required two sets of simulations based on (i) OBCs, corresponding to a finite sample with a boundary, and (ii) PBCs. In case (i) the magnetization $\mathbf{M}$ was computed in the trivial way by means of Eq. (14), while in case (ii) $\mathbf{M}$ was computed by means of Eq. (52), discretized on a numerical grid and exploiting a smearing technique (Fermi-Dirac occupancy at finite $T$). The two sets of computations indeed converged to the *same* $\mathbf{M}$ *value* in the large-system limit [22].

More recently, a quantum derivation of Eq. (52) beyond the semiclassical regime, and based on perturbation theory, was published by Shi et al. [24]. Only one first-principle implementation exists at the time of writing. This is still at the stage of a preprint [28] and concerns the orbital contribution to the spontaneous magnetization of Fe, Co, and Ni.

In order to proceed further, it is expedient to write Eq. (52) identically as the sum of two terms, each of them separately gauge invariant, hence in principle separately measurable

$$\begin{aligned}
\mathbf{M} &= \mathbf{M}_1 + \mathbf{M}_2 \\
\mathbf{M}_1 &= \sum_n \int_{\mathrm{BZ}} d\mathbf{k}\ f_{n\mathbf{k}}\ \mathbf{m}_n(\mathbf{k})\ , \quad \mathbf{m}_n(\mathbf{k}) = \frac{1}{2c(2\pi)^3} \mathrm{Im}\ \langle \partial_{\mathbf{k}} u_{n\mathbf{k}}| \times (\ H_{\mathbf{k}} - \epsilon_{n\mathbf{k}}\ ) |\partial_{\mathbf{k}} u_{n\mathbf{k}}\rangle\ ; \quad (53) \\
\mathbf{M}_2 &= \frac{1}{c(2\pi)^3} \sum_n \int_{\mathrm{BZ}} d\mathbf{k}\ f_{n\mathbf{k}}\ (\ \mu - \epsilon_{n\mathbf{k}}\ )\ \mathbf{\Omega}_n(\mathbf{k})\ . \quad (54)
\end{aligned}$$

Here $\mathbf{\Omega}_n(\mathbf{k})$ is the Berry curvature, Eq. (44), and $\mathbf{m}_n(\mathbf{k})$ coincides with the semiclassical formula for the magnetization of a wavepacket in the $n$-th band [88].

### 8.4 Finite-temperature formula

It has already been stated that—at variance with the electrical analogue **P**—orbital magnetization **M** is a well defined physical property even at nonzero temperature. The Fermi occupancy factor as a function of $\mu$ (chemical potential) and $\beta$ (inverse temperature) becomes

$$f_{n\mathbf{k}} = \frac{1}{\mathrm{e}^{\beta(\epsilon_{n\mathbf{k}}-\mu)}+1}\ . \tag{55}$$

According to Shi et al. [24] the finite-temperature orbital magnetization can be written as $\mathbf{M} = \mathbf{M}_1 + \mathbf{M}_2$, where $\mathbf{M}_1$ is identical in form to Eq. (53), whereas $\mathbf{M}_2$ becomes instead

$$\mathbf{M}_2 = \frac{1}{c(2\pi)^3}\sum_n \int_{\mathrm{BZ}} d\mathbf{k}\ \frac{1}{\beta}\ln\left[1+\mathrm{e}^{-\beta(\epsilon_{n\mathbf{k}}-\mu)}\right]\mathbf{\Omega}_n(\mathbf{k}), \tag{56}$$

whose $T \to 0$ limit coincides with Eq. (54). The formulas given here hold for any crystalline system: normal insulators, Chern insulators, and metals.

Next we take the $\mu$ derivatives of the two terms in the magnetization formula:

$$\frac{\partial \mathbf{M}_1}{\partial \mu} = \sum_n \int_{\mathrm{BZ}} d\mathbf{k}\ \frac{\partial f_{n\mathbf{k}}}{\partial \mu}\ \mathbf{m}_n(\mathbf{k}) \tag{57}$$

$$\frac{\partial \mathbf{M}_2}{\partial \mu} = \frac{1}{c(2\pi)^3}\sum_n \int_{\mathrm{BZ}} d\mathbf{k}\ \ f_{n\mathbf{k}}\ \mathbf{\Omega}_n(\mathbf{k}). \tag{58}$$

We notice that at low temperature $\partial f_{n\mathbf{k}}/\partial\mu$ is essentially a $\delta$ at the Fermi surface, and we analyze the three cases in the $T \to 0$ limit.

(i) For a normal insulator $\mu$ falls in an energy gap and the Berry connection integrates to zero over the BZ. Ergo the magnetization **M** is $\mu$-independent.

(ii) For a Chern insulator $\mu$ falls in a bulk gap, ergo $\partial\mathbf{M}_1/\partial\mu$ vanishes, while $\partial\mathbf{M}_2/\partial\mu$ is quantized and proportional to the Chern invariant, Eq. (43):

$$\frac{\partial \mathbf{M}}{\partial \mu} = -\frac{1}{c(2\pi)^2}\mathbf{C}. \tag{59}$$

The physical interpretation of this equation is best understood in 2d, where the analogue of Eq. (59) reads

$$\frac{\partial M}{\partial \mu} = -\frac{C_1}{2\pi c}, \tag{60}$$

and $C_1$ is the Chern number. We address a finite sample cut from a Chern insulator. Owing to Eq. (2) a macroscopic current of intensity $I = cM$ circulates at the edge of any two-dimensional uniformly magnetized sample, hence Eq. (60) yields

$$\frac{dI}{d\mu} = -\frac{C_1}{2\pi}. \tag{61}$$

The role of chiral edge states is elucidated, for example [97, 98], by considering a vertical strip of width $\ell$, where the currents at the right and left boundaries are $\pm I$. The net current vanishes insofar as $\mu$ is constant throughout the sample. When an electric field **E** is applied across the sample, the right and left chemical potentials differ by $\Delta\mu = E\ell$ and the two edge currents no longer cancel. Our Eq. (61) is consistent with the known quantum-Hall results. In fact,

according to Eq. (61), the net current is $\Delta I \simeq -C_1 \Delta\mu/2\pi$, while the transverse conductivity is defined by $\Delta I = \sigma_{\rm T} E \ell$. We thus arrive at Eq. (46).

Remarkably, the above equations state that the contribution of edge states is indeed a bulk quantity, and can be evaluated in the thermodynamic limit by adopting periodic boundary conditions where the system has no edges. As already observed, this feature may look counterintutitive, but this fascinating behavior has been known for more than 20 years in QHE theory [77, 97].

(iii) In a metal both $\mu$-derivatives contribute. The first term $\partial \mathbf{M}_1/\partial\mu$ is nontopological and has bulk nature. It involves only the states at the Fermi level, and simply measures the magnetization change due to the change in occupation of these bulk states. At variance with this, $\partial \mathbf{M}_2/\partial\mu$ is topological and is related to the contribution of chiral boundary states in a finite sample, very similarly to the Chern-insulator case discussed above.

### 8.5 Transport

In presence of spatial inhomogeneity at a macroscopic scale, the chemical potential acquires an $\mathbf{r}$ dependence: $\mu = \mu(\mathbf{r})$. Since $\partial/\partial r_\beta = \partial\mu/\partial r_\beta \; \partial/\partial\mu$, we write Eq. (2) as

$$\frac{1}{c} j_\alpha = \varepsilon_{\alpha\beta\gamma} \frac{\partial M_\gamma}{\partial r_\beta} = \varepsilon_{\alpha\beta\gamma} \frac{\partial \mu}{\partial r_\beta} \frac{\partial M_\gamma}{\partial \mu}, \tag{62}$$

where $\varepsilon_{\alpha\beta\gamma}$ is the antisymmetric tensor, and now Eqs. (57) and (58) could be used. However, it is argued in Ref. [23] that only $\mathbf{M}_2$ contributes to the *transport* current, where $\mathbf{M}_1$ would contribute an unobservable "magnetization current" [99].

If we transform he Berry curvature from vector to tensor form—Eqs. (44) and (45)—we get $\Omega_{n,\alpha\beta} = \varepsilon_{\alpha\beta\gamma}\Omega_{n,\gamma}$, where $\varepsilon_{\alpha\beta\gamma}$ is the antisymmetric tensor. Eq. (58) yields then

$$\varepsilon_{\alpha\beta\gamma} \frac{\partial M_{2,\gamma}}{\partial \mu} = -\frac{1}{c}\sigma_{\alpha\beta}, \tag{63}$$

where $\sigma_{\alpha\beta}$ is the topological AHE conductivity, Eq. (46). Finally Eq. (62) is rewritten for the transport current as

$$j_\alpha = -\sigma_{\alpha\beta} \frac{\partial \mu}{\partial r_\beta}, \tag{64}$$

which is the familiar conductivity formula, once one identifies $-\nabla\mu$ with the electric field. We remind that this formula only concerns the transverse conductivity (i.e. the antisymmetric part of the conductivity tensor), and neglects extrinsic effects.

### 8.6 Dichroic $f$-sum rule

The differential absorption of left and right circularly polarized light by magnetic materials is known as magnetic circular dichroism. In the past 15 years or so a sum rule for x-ray magnetic circular dichroism (XMCD) has been extensively used at synchrotron facilities to obtain information about orbital magnetism in solids. The relationship between the $\mathbf{M}$ measured via the XCMD sum rule and the $\mathbf{M}$ provided by the modern theory has been addressed in 2008 by Souza and Vanderbilt [25], and will be reviewed here.

A very important caveat is in order at the very beginning. We are going to assume in the following that the KS energies and orbitals—both occupied and empty—provide a faithful excitation spectrum of the crystalline system. Clearly, this is a severe approximation, whose accuracy may be doubtful in many materials. We remind, nonetheless, that even the ground state magnetization is—strictly speaking—beyond reach of standard DFT: see the discussion in Sec. 4. The sum rule discussed here is of course exact for noninteracting electrons.

If we define as $\langle \boldsymbol{\sigma}''_{\rm A} \rangle$ the frequency-integrated XCMD spectrum in vector notation, the main result of Ref. [25] is, in atomic Hartree units,

$$\langle \boldsymbol{\sigma}''_{\rm A} \rangle = \pi c \mathbf{M}_1 \tag{65}$$

where $\mathbf{M}_1$ is given by Eq. (53). In other words, only one of the two (gauge-invariant) terms into which we have partitioned $\mathbf{M}$ is measured by the XMCD spectrum. The term $\mathbf{M}_2$, Eq. (54), is missing; its quantitative importance is unknown.

Eq. (65) is proved for normal insulators only—once more, via a transformation to WFs—although it is possibly valid for Chern insulators and metals as well. In the interpretation of Ref. [25] the XCMD sum rule probes the gauge-invariant part of the self-rotation of the occupied WFs.

# 9 Conclusions

We have reviewed here, on a common ground, both the modern theory of polarization $\mathbf{P}$ and the modern theory of orbital magnetization $\mathbf{M}$. The former theory (or its existence at least) is well known in the $\Psi_{\mathbf{k}}$ community. It is implemented as a standard option in most electronic structure codes [13–18], has revolutionized the theory of ferroelectric and piezoelectric materials [19–21], and starts reaching—although very slowly—the elementary textbooks. The theory of magnetization, instead, is still in its infancy. The very first ab-initio implementations [27,28] are appearing at the time of writing (2009). Previous computations of orbital magnetization in solids have invariantly relied on the uncontrolled muffin-tin approximation.

The modern theories address $\mathbf{P}$ and $\mathbf{M}$ in zero macroscopic fields $\mathbf{E}$ and $\mathbf{B}$. The meaning of this apparently counterintuitive situation is thoroughly discussed (Sec. 2).

The presentation given here is strictly within a KS scheme, whose limitations are however discussed (Sec. 4). We provide formulas both for crystalline solids, where $\mathbf{P}$ and $\mathbf{M}$ are Brillouin-zone integrals (discretized for numerical work), and for noncrystalline condensed systems in a single $\mathbf{k}$-point supercell framework.

At the KS level both theories are in (I dare saying) a definitive shape. Instead, when dealing with explicitly correlated wavefunctions (such as within quantum Monte Carlo), a successful formula exists for $\mathbf{P}$ [6,7]—not discussed here—but not yet for $\mathbf{M}$.

## 10 Acknowledgments

The developments reported in this review cover a period of many years, during which I have profited enormously of discussions with many coworkers and colleagues, too many to be mentioned individually. Here I want to acknowledge explicitly Qian Niu and David Vanderbilt, whose contributions dominate this review. The work in this area has been continuously supported since many years by the Office of Naval Research, thanks to Wally Smith's vision. My current ONR grant is N00014-07-1-1095.

## References

[1] L. D. Landau and E. M. Lifshitz, *Electrodynamics of Continuous Media* (Pergamon Press, Oxford, 1984).

[2] J. D. Jackson, *Classical Electrodynamics* (Wiley, New York, 1975).

[3] M. Posternak, A. Baldereschi, A. Catellani and R. Resta, Phys. Rev. Lett. **64**, 1777 (1990).

[4] R. Resta, Ferroelectrics **136**, 51 (1992).

[5] R. D. King-Smith and D. Vanderbilt, Phys. Rev. B **47**, 1651 (1993).

[6] G. Ortíz and R. M. Martin, Phys. Rev. B **43**, 14202 (1994).

[7] R. Resta, Phys. Rev. Lett. **80**, 1800 (1998).

[8] R. Resta, Rev. Mod. Phys. **66**, 899 (1994).

[9] D. Vanderbilt and R. Resta, in: *Conceptual foundations of materials: A standard model for ground- and excited-state properties*, S.G. Louie and M.L. Cohen, eds. (Elsevier, 2006), p. 139.

[10] R. Resta and D. Vanderbilt, in: *Physics of Ferroelectrics: a Modern Perspective*, Topics in Applied Physics Vol. **105**, Ch. H. Ahn, K. M. Rabe, and J.-M. Triscone, eds. (Springer-Verlag, 2007), p. 31.

[11] D. Xiao, J. Shi, and Q. Niu, Phys. Rev. Lett. **95**, 137204 (2005).

[12] T. Thonhauser, D. Ceresoli, D. Vanderbilt, and R. Resta, Phys. Rev. Lett. **95**, 137205 (2005).

[13] `http://www.abinit.org/`.

[14] `http://www.cpmd.org/`.

[15] `http://www.crystal.unito.it/`.

[16] `http://www.quantum-espresso.org`.

[17] `http://www.uam.es/departamentos/ciencias/fismateriac/siesta/`.

[18] http://cms.mpi.univie.ac.at/vasp/.

[19] R. Resta, Modelling Simul. Mater. Sci. Eng. **11**, R69 (2003).

[20] W. H. Duan and Z. R. Liu, Curr. Opin. Solid State Mater. Sci. **10**, 40 (2006).

[21] M. Rabe, and J.-M. Triscone, eds., *Physics of Ferroelectrics: a Modern Perspective*, Topics in Applied Physics Vol. **105**, Ch. H. Ahn, K. (Springer-Verlag, 2007).

[22] D. Ceresoli, T. Thonhauser, D. Vanderbilt, R. Resta, Phys. Rev. B **74**, 024408 (2006).

[23] D. Xiao, Y. Yao, Z. Fang, and Q. Niu, Phys. Rev. Lett. **97**, 026603 (2006).

[24] J. Shi, G. Vignale, D. Xiao, and Q. Niu, Phys. Rev. Lett. **99** (2008).

[25] I. Souza and D. Vanderbilt, Phys. Rev. B **77**, 054438 (2008).

[26] D. Ceresoli, R. Resta, Phys. Rev. B **76**, 012405 (2007).

[27] T. Thonhauser, D. Ceresoli, A.A. Mostofi, N. Marzari, R. Resta, and D. Vanderbilt, J. Chem. Phys. **131**, 101101 (2009).

[28] D. Ceresoli, U. Gerstmann, A. P. Seitsonen, and F. Mauri, http://arXiv:0904.1988.

[29] http://www.cecam.org/workshop-303.html.

[30] F. Mauri, B. G. Pfrommer, and S. G. Louie, Phys. Rev. Lett. **77**, 5300 (1996).

[31] I. Souza, J. Ìñìguez, and D. Vanderbilt, Phys. Rev. Lett. **89**, 117602 (2002).

[32] P. Umari and A. Pasquarello, Phys. Rev. Lett. **89**, 157602 (2002).

[33] C. Kittel, *Introduction to Solid State Physics*, 7th. edition (Wiley, New York, 1996).

[34] K. Huang, Proc. Roy. Soc. **A203**, 178 (1950).

[35] M. Born and K. Huang, *Dynamical Theory of Crystal Lattices* (Oxford University Press, Oxford, 1954).

[36] N. W. Ashcroft and N. D. Mermin, *Solid State Physics* (Saunders, Philadelphia, 1976).

[37] R. M. Martin, Phys. Rev. B **9**, 1998 (1974).

[38] L. L. Hirst, Rev. Mod. Phys. **69**, 607 (1997).

[39] G. Vignale and M. Rasolt, Phys. Rev. B **37**, 10685 (1988).

[40] H. Ebert, M. Battocletti, and E. K. U. Gross, Europhys. Lett. **40**, 545 (1997).

[41] S. Pittalis, S. Kurth, N. Helbig, and E. K. U. Gross, Phys. Rev. A **74**, 062511 (2006).

[42] S. Sharma, S. Pittalis, S. Kurth, S. Shallcross, J. K. Dewhurst, and E. K. U. Gross, Phys. Rev. B **76**, 100401 (2006).

[43] X. Gonze, Ph. Ghosez, and R. W. Godby, Phys. Rev. Lett. **74**, 4035 (1995).

[44] S. J. A. van Gisbergen, F. Koostra, P. R. T. Schipper, O. V. Gritsenko, J. G. Snijders, and E. J. Baerends, Phys. Rev. A **57**, 2556 (1998).

[45] F. Mauri and S. G. Louie, Phys. Rev. Lett. **76**, 4246 (1996).

[46] C. J. Pickard and F. Mauri, Phys. Rev. B **63**, 245101 (2001); Phys. Rev. Lett. **91**, 196401 (2003).

[47] M. A. L. Marques, M. d'Avezac, and F. Mauri, Phys. Rev. B **73**, 125433 (2006).

[48] J. R. Yates, C. J. Pickard, and F. Mauri, Phys. Rev. B **76**, 024401 (2007).

[49] R. Resta, M. Posternak, and A. Baldereschi, Phys. Rev. Lett. **70**, 1010 (1993).

[50] A. Pasquarello and R. Car, Phys. Rev. Lett. **79**, 1766 (1997).

[51] P. L. Silvestrelli, M. Bernasconi, and M. Parrinello, Chem. Phys. Lett. **277**, 478 (1997).

[52] M. Sharma, R. Resta, R. Car, Phys. Rev. Lett. **95**, 187401 (2005).

[53] S. Picozzi and C. Ederer, `http://www.psi-k.org/newsletters/News_92/Highlight_92.pdf`.

[54] A. M. Essin, J. E. Moore, and D. Vanderbilt, Phys. Rev. Lett. **102**, 146805 (2009).

[55] R. M. Martin, Phys. Rev. B **5**, 1607 (1972).

[56] R. Car and M. Parrinello, Phys. Rev. Lett. **55**, 2471 (1985).

[57] S. Baroni and R. Resta, Phys. Rev. B **33**, 7017 (1986).

[58] S. de Gironcoli, S. Baroni, and R. Resta, Phys. Rev. Lett. **62**, 2853 (1989).

[59] S. Baroni, S. de Gironcoli, A. Dal Corso, and P. Giannozzi, Rev. Mod. Phys. **73**, 515 (2001).

[60] X. Wu, D. Vanderbilt, and D. Hamann, Phys. Rev. B **72**, 035105 (2005).

[61] S. Massidda, R. Resta, M. Posternak, and A. Baldereschi, Phys. Rev. B **52** 16977 (1995).

[62] S. Massidda, M Posternak, A. Baldereschi, and R. Resta, Phys. Rev. Lett. **82**, 430 (1999).

[63] C. J. Pickard and F. Mauri, Phys. Rev. Lett. **88**, 086403 (2002).

[64] *Encyclopedia of NMR*, edited by D.M. Grant and R.K. Harris (Wiley, London, 1996).

[65] I. I. Rabi, J. R. Zacharias, S. Millman, and P. Kusch, Phys. Rev. **53**, 318 (1938).

[66] D. Sebastiani and M. Parrinello, J. Phys. Chem. A **105**, 1951 (2001).

[67] D. Sebastiani and M. Parrinello, , ChemPhysChem **3**, 675 (2002).

[68] B. G. Pfrommer, F. Mauri, and S. G. Louie, J. Am. Chem. Soc. **122**, 123 (2000).

[69] R. Resta, Int. J. Quantum Chem. **75**, 599 (1999).

[70] R. Resta, J. Phys.: Condens. Matter **12**, R107 (2000).

[71] A. Pasquarello and R. Resta, Phys. Rev. B **68**, 174302 (2003).

[72] G. H. Wannier, Phys. Rev. **52**, 191 (1937).

[73] N. Marzari and D. Vanderbilt, Phys. Rev. B **56**, 12847 (1997).

[74] N. Marzari, I. Souza, and D. Vanderbilt, `http://www.psi-k.org/newsletters/News_57/Highlight_57.pdf`.

[75] R. Resta, J. Chem. Phys. **124**, 104104 (2006).

[76] E. I. Blount, in *Solid State Physics*, edited by H. Ehrenreich, F. Seitz and D. Turnbull, vol **13** (Academic, New York, 1962), p. 305.

[77] D. J. Thouless, M. Kohmoto, M. P. Nightingale, and M. den Nijs, Phys. Rev. Lett. **49**, 405 (1982).

[78] Q. Niu, D. J. Thouless, and Y. S. Wu, Phys. Rev. B **31**, 3372 (1985).

[79] D. J. Thouless, *Topological Quantum Numbers in Nonrelativistic Physics* (World Scientific, Singapore, 1998).

[80] F. D. M. Haldane, Phys. Rev. Lett. **61**, 2015 (1988).

[81] T. Thonhauser and D. Vanderbilt, Phys. Rev. B **74**, 235111 (2006).

[82] M. Taillefumier, V. K. Dugaev, B. Canals, C. Lacroix, and P. Bruno, Phys. Ref. B **78**, 155330 (2008).

[83] C. L. Kane and E. J. Mele, Phys. Rev. Lett. **95**, 226801 (2005).

[84] D. N. Sheng, Z. Y. Weng, L. Sheng, and F. D. M. Haldane, Phys. Rev. Lett. **97**, 036808 (2006).

[85] S.-C. Zhang, Physics **1**, 6 (2008).

[86] Y. L. Chen et al., Science **325**, 178 (2009).

[87] J. E. Moore, Physics **2**, 82 (2009).

[88] G. Sundaram and Q. Niu, Phys. Rev. B **59**, 14915 (1999).

[89] R. Karplus and J. M. Luttinger, Phys. Rev. **95**, 1154 (1954).

[90] T. Jungwirth, Q. Niu, and A. H MacDonald, Phys. Rev. Lett. **88**, 207208 (2002).

[91] Z. Fang *et al.*, Science **301**, 92 (2003).

[92] Y. Yao, L. Kleinman, A. H. MacDonald, J. Sinova, T. Jungwirth, D.-S. Wang, E. Wang, and Q. Niu, Phys. Rev. Lett. **92**, 037204 (2004).

[93] X. Wang, D. Vanderbilt, J. R. Yates, and I. Souza, Phys. Rev. B **76**, 195109 (2007).

[94] O. Gat and J. E. Avron, New J. Phys. **5**, 44 (2003).

[95] N. Sai, K. M. Rabe, and D. Vanderbilt, Phys. Rev. B **66**, 104108 (2002).

[96] I. Souza, J. Íñiguez and D. Vanderbilt, Phys. Rev. B **69**, 085106 (2004).

[97] B. I. Halperin, Phys. Rev. B **25**, 2185 (1982).

[98] D. Yoshioka, *The Quantum Hall Effect* (Springer, Berlin, 2002).

[99] N. R. Cooper, B. I. Halperin, and I. M. Ruzin, Phys. Rev. B **55**, 2344 (1997).